

UCSF

UC San Francisco Electronic Theses and Dissertations

Title

Oncogenic signaling regulation of the mutant TERT promoter

Permalink

<https://escholarship.org/uc/item/8520r6d9>

Author

Mckinney, Andrew

Publication Date

2022

Peer reviewed|Thesis/dissertation

Oncogenic signaling regulation of the mutant TERT promoter

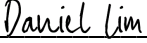
by
Andrew McKinney

DISSERTATION
Submitted in partial satisfaction of the requirements for degree of
DOCTOR OF PHILOSOPHY

in
Biomedical Sciences

in the
GRADUATE DIVISION
of the
UNIVERSITY OF CALIFORNIA, SAN FRANCISCO

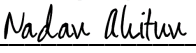
Approved:

DocuSigned by:

FC7A2B6D45EF428... Daniel Lim
Chair

DocuSigned by:

Joseph Costello

DocuSigned by:
Russell Pieper
Russell Pieper

DocuSigned by:

77BA96E7DAE34F4... Nadav Ahituv

Committee Members

To my parents, Tim and Andrene, and my wife, Adrienne

For your unconditional support and love

Oncogenic Signaling Regulation of the Mutant TERT Promoter

Andrew McKinney

ABSTRACT

Telomerase activation counteracts senescence and death-inducing telomere erosion caused by uncontrolled proliferation in cancer. Proliferation is highly correlated with telomerase activity across cancer types, suggesting there may be a mechanism linking these cancer hallmarks. In two of the major classes of adult diffuse glioma, high grade glioblastoma and low grade oligodendroglioma, telomerase reverse transcriptase promoter (*TERT*_p) mutations are a predominant alteration underlying telomerase reactivation through recruitment of GA-binding protein (GABP). Very little is known about the mechanisms connecting drivers of proliferation to telomere maintenance and mutant *TERT*_p regulation particularly in glioma. Epidermal growth factor receptor (EGFR) is commonly amplified in glioblastoma driving cell proliferation. *EGFR* amplification and *TERT*_p mutations are frequent and significantly co-occur in glioblastoma. Oligodendroglioma lack *EGFR* amplification, but commonly rely on *CIC* mutations which modulate signaling downstream of receptor tyrosine kinase signaling. To determine if these two signaling pathways are functionally connected to mutant *TERT*_p regulation in glioma, we combined analyses of copy number, mRNA, and protein data from primary tumor tissue with clinical pharmacologic treatments and genetic perturbations in cell lines and patient-derived cultures. From these data, we demonstrate that proliferation arrest lowers *TERT* expression in a GABP-dependent

manner. We elucidate a proliferation-to-immortality pathway from EGFR to increased expression from the mutant *TERT*_p through activation of AMP-mediated kinase (AMPK) and subsequent GABP upregulation. We demonstrate the phenotypic consequences of EGFR-AMPK on promoting telomerase activity and telomere length. These results implicate GABP as a direct link between proliferation signals and telomerase reactivation that is specific to *TERT*_p mutant glioblastoma. In oligodendroglioma, we demonstrate that CIC inactivation upregulates *TERT* from the mutant *TERT*_p through E24 transformation-specific (ETS) factors other than GABP, showing that mechanisms driving proliferation can simultaneously upregulate the mutant *TERT*_p in a cancer-type specific manner.

TABLE OF CONTENTS

CHAPTER 1: INTRODUCTION.....	1
Adult Diffuse Glioma.....	2
<i>Etiology.....</i>	<i>2</i>
<i>Treatments and Outcomes.....</i>	<i>3</i>
Telomere Maintenance, Immortality, and Telomerase.....	3
TERT Promoter Mutations.....	4
 CHAPTER 2: GABP LINKS PROLIFERATION AND TELOMERE MAINTENANCE	
MECHANISMS.....	9
Introduction.....	10
Results.....	10
Discussion.....	12
 CHAPTER 3: EGFR-AMPK SIGNALING STIMULATES TERT EXPRESSION	
FROM THE MUTANT TERT PROMOTER.....	18
Introduction.....	19
Results.....	20
Discussion.....	28
 CHAPTER 4: CIC INACTIVATION STIMULATES THE TERT PROMOTER IN	
OLIGODENDROGLIOMA.....	49
Introduction.....	50

Results	50
Discussion	52
CHAPTER 5: CONCLUSIONS.....	55
CHAPTER 6: MATERIALS AND METHODS.....	60
REFERENCES	71

LIST OF FIGURES

Figure 1.1 Molecular classification of adult diffuse glioma	7
Figure 1.2 Schematic of GABP heterotetramer binding to the mutant <i>TERT</i> _p	8
Figure 2.1 <i>TERT</i> expression is associated with proliferation in human cancer	14
Figure 2.2 GABP links proliferation to mutant <i>TERT</i> _p activity and telomerase activity.....	17
Figure 3.1 <i>TERT</i> expression correlates with <i>EGFR</i> amplification and <i>EGFR</i> expression in human GBM	30
Figure 3.2 <i>EGFR</i> signaling selectively upregulates the mutant <i>TERT</i> _p	32
Figure 3.3 Pharmacological inhibition of <i>EGFR</i> downregulates the <i>GABP-TERT</i> axis.....	33
Figure 3.4 <i>EGFR</i> signaling upregulates the mutant <i>TERT</i> _p by increasing <i>GABP</i> expression.....	35
Figure 3.5 <i>GABP</i> and p- <i>AMPK</i> are elevated in <i>EGFR</i> -high GBM	36
Figure 3.6 Activated <i>AMPK</i> upregulates <i>GABP</i> subunit expression downstream of <i>EGFR</i>	38
Figure 3.7 <i>PRKAB1</i> correlates with <i>GABP</i> subunit expression in GBM.....	40
Figure 3.8 CRISPR-mediated full gene knockout of <i>PRKAB1</i> reduces <i>GABP</i> and <i>TERT</i>	41
Figure 3.9 <i>AMPK</i> signaling selectively regulates the mutant <i>TERT</i> _p	43
Figure 3.10 The <i>EGFR-AMPK</i> axis regulates telomerase activity and telomere length in <i>TERT</i> _p mutant GBM.....	44

Figure 3.11 <i>EGFR</i> or <i>PRKAB1</i> inhibition slows cell doubling time.....	46
Figure 3.12 <i>EGFR</i> overexpression counteracts telomere shortening from <i>TERT</i> knockdown.....	47
Figure 4.1 <i>CIC</i> mutant tumors express higher <i>TERT</i> and ETS factors.....	53
Figure 4.2 <i>CIC</i> regulates the mutant <i>TERT</i> _p through ETS regulation	54

LIST OF TABLES

Table 1.1 List of Reagents and Primers Used.....	69
--	----

CHAPTER 1: INTRODUCTION

Adult Diffuse Glioma

Etiology

Adult diffuse glioma is the most common class of adult brain tumor, occurring in 4.67 to 5.73 persons per 100,000 in 2014 (Ostrom et al., 2014). Originally classified by histological and limited immunohistochemistry markers, the 2016 World Health Organization incorporated molecular features which are now used to define glioma subtypes. The 2021 World Health Organization guidelines delineate three main types of adult glioma—astrocytoma, oligodendroglioma, and glioblastoma (GBM) (**Figure 1.1**). Astrocytoma comprise grade I and II (low grade glioma) and can progress to grade III or IV (high grade). Oligodendroglioma comprise grade II (low grade), or grade III (high grade). Grade IV GBM can arise either *de novo* as a primary GBM or as a recurrence from low grade glioma. Oligodendroglioma and low grade astrocytoma occur in younger patients, peaking in 36-44 age group, while high grade astrocytoma and primary GBM occur more commonly in the older 75-84 age group (Ostrom et al. 2014). Astrocytoma and oligodendroglioma harbor mutations in *isocitrate dehydrogenase 1 or 2 (IDH1 or IDH2)* and are distinguished by the 1p/19q co-deletion which is unique to oligodendroglioma. Astrocytoma commonly harbors *alpha-thalassemia/mental retardation, X-linked (ATRX)* and *tumor protein p53 (TP53)* mutations, while oligodendroglioma harbors *capicua (CIC)* or *far upstream element binding protein 1 (FUBP1)* mutations. Primary GBM are defined by the absence of IDH mutations and combined chromosome 7 gain and chromosome 10 loss (Louis et al. 2016).

Treatments and Outcomes

Prognosis for patients with primary GBM is poor, with median survival of 15 months (Louis et al, 2016), while low grade glioma patients have an average survival of 7 years. Standard of care for low grade glioma is gross total resection and concomitant treatment with radiotherapy and the chemotherapeutic agent temozolomide, while in GBM treatment, tumor treating fields are sometimes applied in addition to resection and temozolomide (Stupp et al, 2017). Beyond these treatments, few advances have been made in treatment of these diseases over the last 50 years, highlighting the need for novel therapeutic paradigms.

Telomere Maintenance, Immortality, and Telomerase

The ends of chromosomes shorten progressively across cell divisions due to the inefficiency of DNA polymerase in lagging strand synthesis. Telomere repeats of TTAGGG are added to the end of chromosomes to offset this shortening (Greider and Blackburn, 1985). Telomeres are maintained at a length of 5 to 15 kilobases in normal human cells, though there is substantial heterogeneity within cell types and within individual chromosomes of a single cell (Whittemore et al, 2019; Lansdorp et al 1996). Telomeres are bound by proteins termed the shelterin complex, which caps and protects chromosome ends from being recognized as DNA double stranded breaks (Takai et al, 2003). If cells fail to extend telomeres and ultimately reach a critically short telomere length the shelterin complex can no longer bind, triggering the DNA damage response. Cells then enter senescence in a p53- and Rb-mediated manner and

eventually activate cell death pathways, most notably apoptosis (Saretzki et al, 1999). Telomere shortening restricts the lifespan of somatic cells, however stem and germ cells which must continually divide require a mechanism of telomere maintenance.

The ribonucleoprotein complex telomerase adds telomeric repeats to the end of chromosomes. Telomerase is composed of the enzymatic subunit TERT and the RNA template encoded by telomerase RNA component (*TERC*). The template RNA strand binds to the 3' overhang of the telomere and the reverse transcriptase subunit adds additional telomeric units, which allows DNA polymerase to synthesize the complementary strand (Feng et al 1995). Telomerase is silenced in most somatic adult cells through repression of *TERT* transcription to limit cellular lifespan, and re-expression is sufficient to lengthen telomers and achieve cellular immortality. Cancer cells are highly proliferative and therefore must have active telomere maintenance mechanisms to counteract telomere attrition. Over 90% of cancers achieve this through re-expression of *TERT* (Kim et al. 1994; Shay and Bacchetti 1997).

TERT Promoter Mutations

The mechanism of *TERT* re-activation has been unclear or entirely unexplained for many tumors. Several mechanisms have been described, from MYCN amplification (Huang et al, 2020) to structural rearrangements of *TERT* (Peifer et al, 2015) and expression of proteins from onco-viruses such as HBV (Bellon and Nicot, 2008), but these account for only a small subset of cancers. In over 50 types of cancer, telomerase is reactivated through a mutation in the promoter of *TERT*. *TERT*_p mutations are the most common non-coding mutations in cancer, including over 80% of IDH1 wildtype

(*IDH1*-WT) primary GBM (Huang et al. 2013; Horn et al. 2013; Remke et al. 2013; Quass et al 2014; Zehir et al 2017; Killela et al. 2013; Aquilanti et al 2021; Vinagre et al. 2013; Arita et al, 2013; Patel et al, 2020). Two mutations, C228T and C250T, occur in a mutually exclusive fashion. C228T occurs more commonly than C250T, but both are associated with elevated *TERT* expression (Huang et al 2013, Spiegl-Kreinecker et al 2015).

*TERT*_p mutations create an identical GGAA binding site for the ETS class of transcription factors. A comprehensive screen of the ETS factors expressed in glioma identified GA-binding protein (GABP) as the primary transcription factor responsible for binding to and activating the mutant *TERT*_p across multiple *TERT*_p mutant cancers (Bell et al, 2015). GABP is the only ETS factor that acts as an obligate multimer and is composed of the DNA-binding subunit GABPA and the transactivating subunit GABPB1 (**Figure 1.2**, Bell et al, 2016). GABPB1 has a long (GABPB1L) and a short isoform (GABPB1S). GABPB1L forms heterotetramers with GABPA, while GABPB1S exclusively forms heterodimers (de la Brousse et al, 1994). The heterotetrameric form of GABP was demonstrated to bind to the mutant *TERT*_p through use of one de novo ETS site created by the promoter mutation and one native site in the promoter (Mancini et al, 2018). Genetic modification of GABP by CRISPR-mediated insertion/deletions led to a reversal of cellular immortality in vitro and reduced tumor growth in vivo (Mancini et al 2018). Meanwhile, using an inducible system *in vivo*, it was shown that GABP reduction combined with temozolomide, a standard of care for GBM patients, reduced cellular proliferation and dramatically prolonged survival of mice bearing *MGMT* methylated

GBM, highlighting the therapeutic potential of targeting the GABP-*TERT* axis (Amen et al 2021).

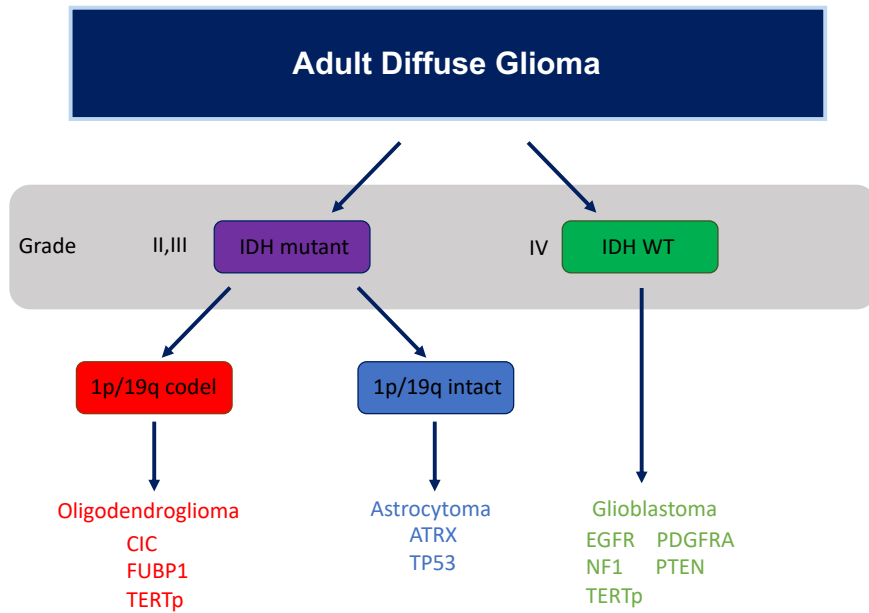


Figure 1.1 Molecular classification of adult diffuse glioma

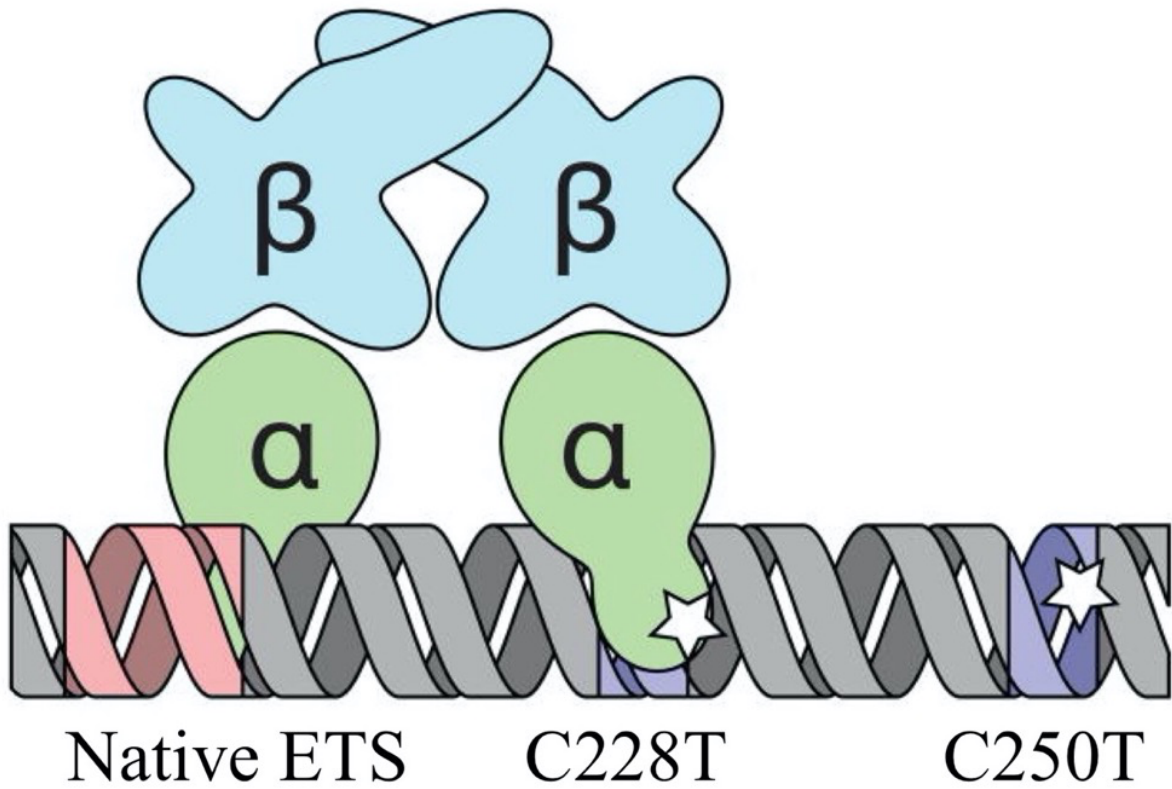


Figure 1.2 Schematic of GABP heterotetramer binding to the mutant *TERTp*

CHAPTER 2: GABP LINKS PROLIFERATION AND TELOMERE MAINTENANCE MECHANISMS

Introduction

In rapidly dividing tumor cells, the *TERT*_p mutation alone may not be sufficiently activating to maintain telomere length and may require additional input (Chiba et al 2015). Telomerase is expressed in proliferating but not quiescent cancer cells, with levels remaining constant throughout the cell cycle (Holt et al 1996; Kyo et al 1997; Holt et al 1997). A multi-gene expression signature approximating telomerase activity has been positively associated with proliferation in cancer samples (Noureen et al 2021). Together, this raises the possibility of a functional connection between proliferation and telomerase.

Results

Examining the 31 cancer types profiled in TCGA, including *TERT*_p WT and *TERT*_p mutant tumors, we observed that *TERT* expression was significantly positively associated with *MKI67* expression, a marker of actively cycling cells that is absent in cells in the G0 phase of the cell cycle (**Figure 2.1A**). In *IDH1*-WT GBM, the majority of which are *TERT*_p mutant, a similar correlation is observed (**Figure 2.1B**).

Telomerase is significantly lower in quiescent tumor cells than in proliferating cells, but it is unclear how proliferation influences *TERT* expression in *TERT*_p mutant cells (Holt et al 1997). To test for effects of proliferation on the mutant *TERT*_p, we serum starved *TERT*_p mutant GBM cells to arrest proliferation (**Figure 2.1C**). After one day of starvation, *TERT* expression and telomerase activity were reduced in *TERT*_p mutant GBM cell lines including the patient-derived line SF7996, as well as in *TERT*_p wild type GBM cell lines (**Figure 2.2A-B**). To test if the link between proliferation and mutant

*TERT*_p regulation is unique to GBM or more generalizable, we further serum starved 13 cell lines representing the seven most common *TERT*_p mutant cancers and observed reduced *TERT* expression in 12 of 13 lines, indicating that the relationship between *TERT* expression and proliferation is not unique to GBM (**Figure 2.1D**). In mouse embryonic fibroblasts, *Gabpa* and *Gabpb1* are expressed at lower levels in serum-starved cells than serum-stimulated cells (Yang et al 2007). We therefore hypothesized that changes in GABPA and GABPB1 could underlie the relationship between cell proliferation and regulation of *TERT* in *TERT*_p mutant cancers.

Indeed, GABPA and GABPB1 expression were decreased in both *TERT*_p mutant and *TERT*_p wildtype GBM cells upon serum starvation. Chromatin immunoprecipitation experiments revealed that overall reduction in GABP levels was accompanied by a specific reduction of GABP occupancy at the *TERT*_p in *TERT*_p mutant GBM cells (**Figure 2.2C-D**). Importantly, serum starvation induces numerous cellular and molecular changes, many of which could contribute to *TERT* reduction. We therefore sought to determine if *GABPA* and *GABPB1* expression is sufficient to rescue *TERT* expression upon serum starvation. We expressed ectopic *GABPA* and *GABPB1* simultaneously and observed a rescue of basal *TERT* expression and telomerase activity in *TERT*_p mutant cells despite serum starvation (**Figure 2.2E-G**). *TERT* expression did not increase significantly in non-starved cells upon ectopic expression of *GABPA* and *GABPB1*, suggesting that GABP is not rate-limiting when cells are grown at standard 10% serum concentrations. In contrast to the clear rescue of *TERT* expression, ectopic expression of *GABPA* and *GABPB1* did not rescue proliferation caused by serum starvation (**Figure 2.1E**). Therefore, the rescue of *TERT* expression

cannot be attributed to an indirect effect from increased proliferation. Importantly, rescue of *TERT* expression and telomerase activity was not observed in *TERT*_p WT cells (**Figure 2.2F-G**). It is unclear by which mechanism proliferation regulates *TERT* in the *TERT*_p WT setting. However, GABP links cell proliferation and *TERT* expression selectively in *TERT*_p mutant tumor cells.

Discussion

Regulators of the mutant *TERT*_p serve as intriguing therapeutic targets as *TERT*_p mutations are usually early, clonal events in the vast majority. These findings suggest that an added benefit of targeting drivers of tumor cell proliferation could be reducing *TERT* expression in addition to slowing growth. Telomere length may be unaffected by reduction of *TERT* if accompanied by a reduction in proliferation—therefore, direct telomere targeting methods such as drugs targeting the shelterin complex could be used in quiescent cells to induce telomeric damage without telomerase present to counteract the shortening that occurs.

GABP is necessary and sufficient for exit from *G0* and entry into the cell cycle in mouse embryonic fibroblast cells (Yang et al 2007). GABP expression in the cell cycle therefore is reminiscent of telomerase expression patterns, which is also specifically upregulated upon exit from quiescence and entry into the cell cycle. Here, we demonstrate that GABP is a link between proliferation and telomerase activity in the *TERT*_p mutant context. Given *TERT*_p WT cells also exhibit lower telomerase when quiescent, other transcriptional regulators of *TERT* may be affected by exit from the cell cycle. Myc is a regulator of the *TERT*_p and is also upregulated upon exit from

quiescence, which could provide one avenue of further study in large number of *TERT*^p wild type, *TERT* expressing cancers (Helbing et al, 1998).

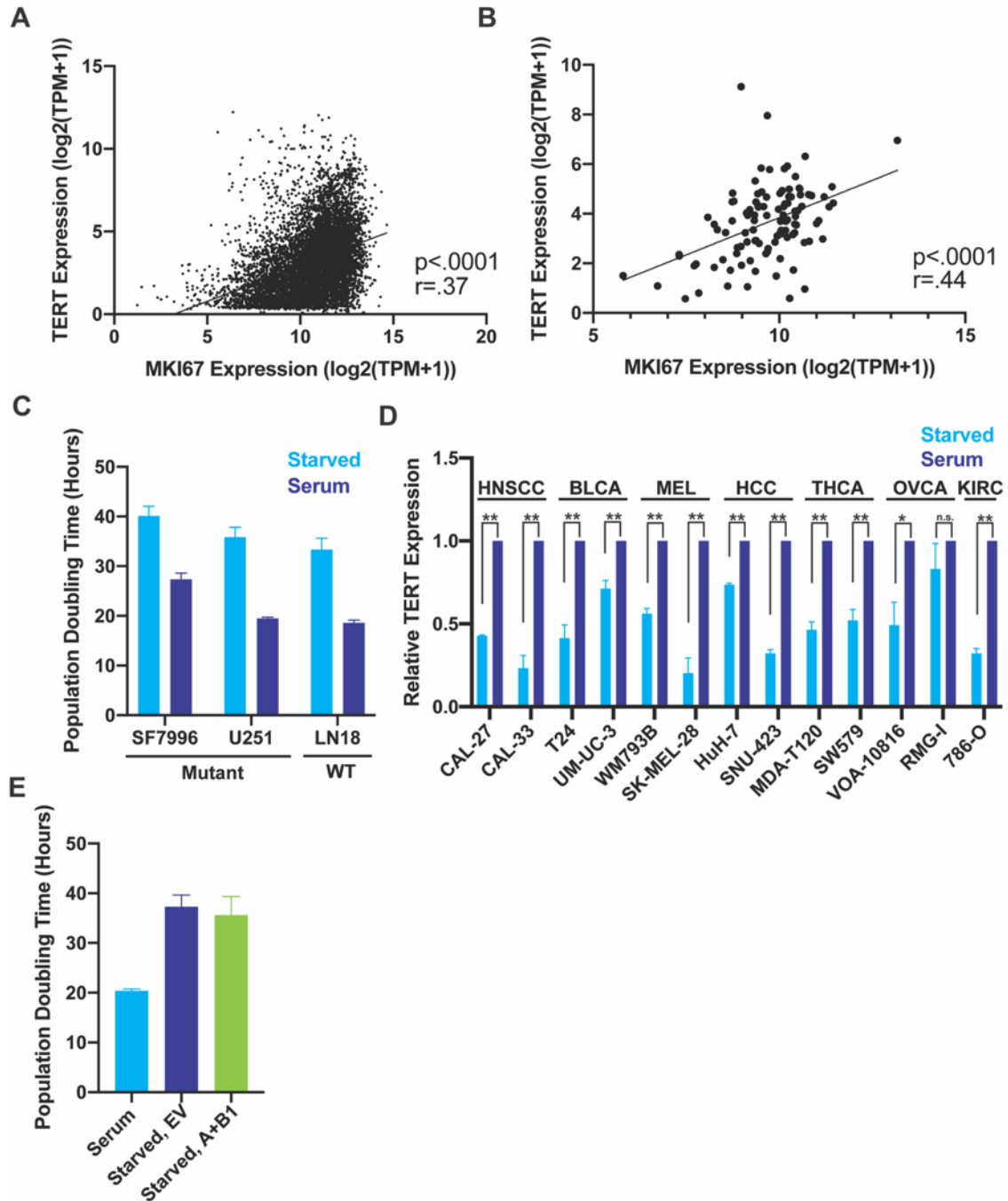


Figure 2.1 *TERT* expression is associated with proliferation in human cancer

(A-B) Correlation of *MKI67* and *TERT* expression from RNA-Seq of 8341 tumors from 31 cancer types (A) and *IDH1*-WT GBM of 106 tumors (B) tumors from TCGA . r, Pearson correlation coefficient, $p < 0.0001$. (C) Population doubling after 24 hours of serum starvation in LN18, U251, SF7996 cells. (D) *TERT* expression following 24 hours

serum induction after serum starvation of *TERT*^p-mut cells after in head and neck squamous cell carcinoma (HNSCC), urinary bladder cancer (BLCA), melanoma (MEL), hepatocellular carcinoma (HCC), thyroid cancer (THCA), ovarian cancer (OVCA), and renal cell carcinoma (KIRC). (E) Population doubling after 24 hours serum starvation in U251 cells expressing ectopic *GABPA* and *GABPB1* (A + B1) or empty vector (EV) control.

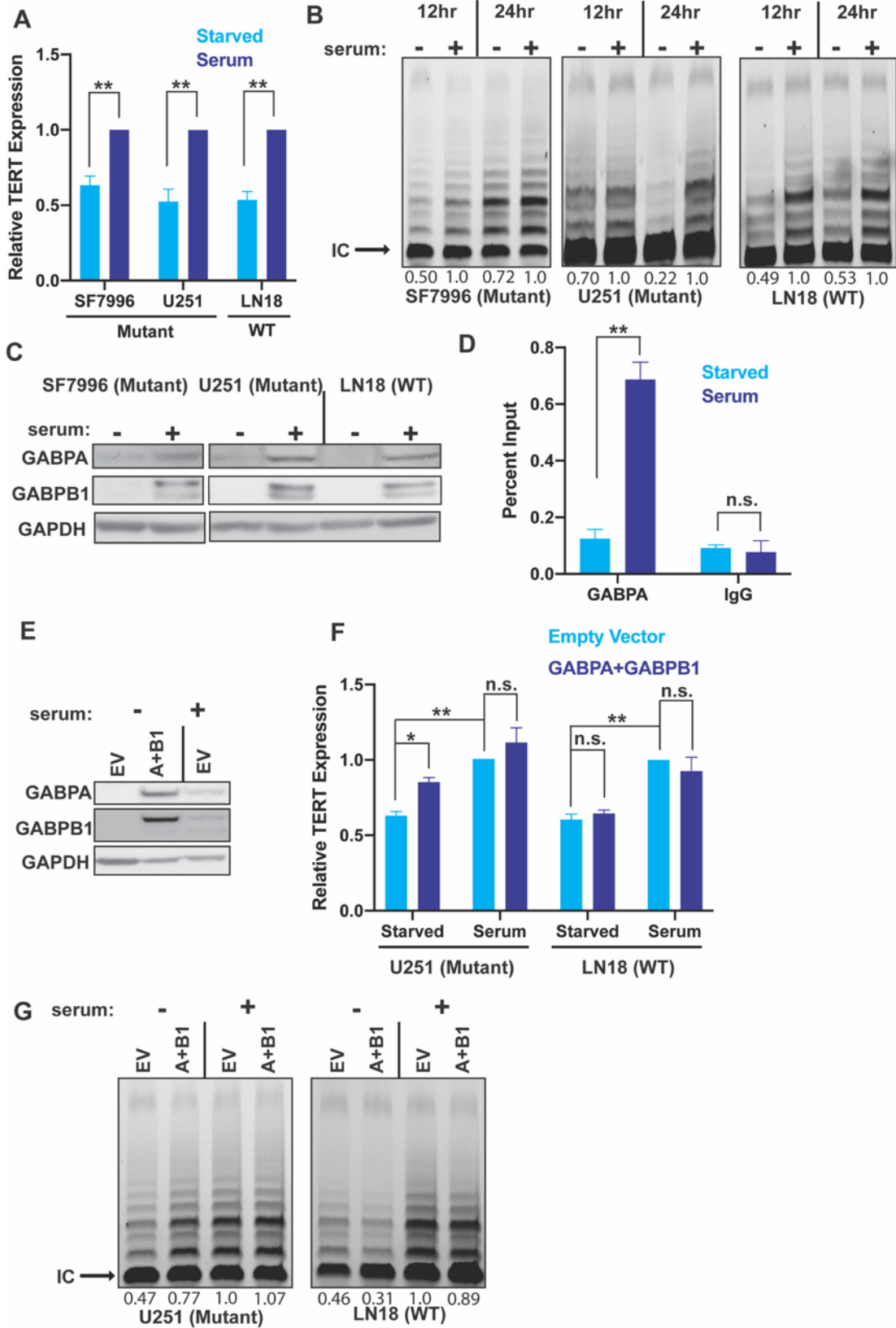


Figure 2.2 GABP links proliferation to mutant *TERT*_p activity and telomerase activity

(A) *TERT* expression in serum starved cells after 24 hours serum induction. (B) Telomerase activity in cells starved for 12 or 24 hours, normalized relative to internal control band (IC) to serum condition for each timepoint. (C) Immunoblots in serum starved cells after 24 hours serum induction (D) GABPA ChIP-qPCR for the *TERT*_p in serum starved U251 cells after 24 hours serum induction. (E) Immunoblots in U251 cells upon serum starvation with or without expression of ectopic *GABPA* and *GABPB1*. (F) *TERT* expression in cells expressing ectopic *GABPA* and *GABPB1* with or without serum starvation. (G) Telomerase activity in cells expressing ectopic *GABPA* and *GABPB1* with or without serum starvation normalized relative to internal control band (IC). (A-F), Student's t-tests, two-tailed. *P<0.05, **P<.005, data represent mean +/- SEM.

**CHAPTER 3: EGFR-AMPK SIGNALING STIMULATES *TERT*
EXPRESSION FROM THE MUTANT *TERT* PROMOTER**

Introduction

While oncogenic drivers influence *TERT* expression (Maida et al 2002; Hoffmeyer et al 2012; Bermudez et al 2008; Kyo et al 1999; Cha et al 2008; Hsu et al 2015; Obha et al 2016), in most cancers the mechanisms by which they influence *TERT* expression and whether the influence is specific to the mutant *TERT*_p is poorly understood. One of the first examples was BRAFV600E signaling which leads to mutation-specific *TERT* upregulation through modulation of expression of the ETS factors ETS1 or GABP (Gabler et al 2019; Vallarelli et al 2016; Liu et al 2018; Li et al 2016). The BRAFV600E mutation is exceptionally rare in *TERT*_p mutant GBM however, leaving open the question of which signaling pathways in this highly proliferative tumor might serve a similar function.

EGFR is activated in 57% of GBM through mutation, structural rearrangement and/or focal amplification (Brennan et al 2013). *EGFR* amplification or *TERT*_p mutations are indicators of poor prognosis in GBM (Simon et al 2015; Eckel-Passow et al 2015; Labussière et al 2014; Wijnenga et al 2017; Aibaidula et al 2017; Spiegl-Kreinecker et al 2015). Previous studies have identified a significant co-occurrence of two genomic alterations, *EGFR* amplification and *TERT*_p mutation, in two cohorts of 51 and 395 *IDH1*-WT GBM. In contrast, there is no significant co-occurrence between *TERT*_p and other classical GBM alterations such as *TP53* mutation and *CDKN2A* deletion (Killela et al 2013; Labussière et al 2014). Given these associations, we explored whether signaling from EGFR, which drives cell proliferation among other activities, might be functionally linked to mutant *TERT*_p activity and telomere-related phenotypes in GBM, allowing cells to maintain telomere length when cell proliferation is increased.

Results

Using an independent cohort of 265 tumors from the MSK-IMPACT study, we independently validated the co-occurrence between *EGFR* amplification and *TERT*_p mutation, finding that 94% of *EGFR* amplified samples harbor *TERT*_p mutations (**Figure 3.1A**) (Zehir et al 2017). In contrast, less than 1% (1/110) of *EGFR* amplified samples exhibited *ATRX* loss-of-function mutation indicative of alternative lengthening of telomeres (**Figure 3.1B**). Thus, *EGFR* amplification preferentially occurs in the tumors with *TERT*_p mutation.

To explore this association between the mutant *TERT*_p and *EGFR* beyond the genomic level, we compared their expression at the mRNA and protein levels in multiple GBM datasets. First, in the 129 *IDH1*-WT GBM from TCGA, *TERT* mRNA is significantly higher in tumors with an *EGFR* amplification compared to those without (**Figure 3.1C**). Second, stratifying the 54 TCGA GBM with reverse phase protein array (RPPA) data by their level of *EGFR* activation, as measured by phosphorylation of *EGFR* Y1068 (Rojas et al 1996), shows that a high level of *EGFR* activation is associated with greater *TERT* expression (**Figure 3.2A**). As a complementary approach to the large TCGA cohort with single samples per patient, we examined cases from our UCSF cohort with a relatively large number of samples per tumor. Unlike the TCGA cohort, the intratumoral comparison controls for the strong, potentially confounding differences in genetic background and truncal somatic mutations between different patients. In this analysis, we examined exome and RNA sequencing data from 33 spatially mapped tumor samples from a total of four tumors with one or more samples with *EGFR* amplification and *TERT*_p mutation to maximize sampling of tumor heterogeneity (**Figure 3.1D**,

Supplementary Video 1 and 2). Despite high tumor cell content in all samples, the level of *EGFR* amplification and expression was heterogenous among samples from the same patient, allowing us to test for correlations. Within each of the four tumors, *EGFR* expression positively correlated with *TERT* expression. Statistical significance was reached in two of the four patients. The other two patients had fewer samples and a more narrow range of expression for *TERT* and *EGFR* (**Figure 3.1E**). Importantly, a single sample from Patient 454 that has no detectable *EGFR* amplification also displayed the lowest *TERT* expression. From these diverse inter- and intratumoral data sets, we conclude that *EGFR* amplification is associated with elevated *TERT* expression in *TERT*_p mutant tumors.

Given the associations between elevated *EGFR* mRNA and protein phosphorylation levels, *TERT*_p mutation and *TERT* expression in tumor tissue from GBM patients, we tested for a potentially causal relationship using three independent experimental approaches. First, we utilized EGFRvIII, a common variant detected in ~20% of GBM overall and about half of the GBM cases with amplified *EGFR* (Brennan et al 2013). We expressed ectopic EGFRvIII, which exhibits constitutive ligand-independent activity (Batra et al 1995; Huang et al 1997), in an inducible manner in *TERT*_p mutant U251 cells and observed a rapid and significant increase in *TERT* expression (**Figure 3.2B**). Second, we stimulated endogenous EGFR with EGF ligand, which also caused a significant increase in *TERT* expression (**Figure 3.2C**). These studies support a causal relationship but without additional experiments cannot definitively show selectivity for the mutant promoter since the wildtype promoter is transcriptionally silenced. Therefore, our third approach utilized WT and mutant *TERT*_p

luciferase promoter assays in an isogenic background EGFRvIII overexpression drove *TERT*_p activity to a much higher level and in a mutation-specific manner, increasing reporter activity from a promoter with either the C228T or C250T mutation while not significantly altering activity of the wildtype *TERT*_p (**Figure 3.2D**). Overexpression studies typically produce non-physiologic levels of the expressed protein however the expression level of the ectopic EGFR may be closer to physiologic levels for EGFR amplified tumors. To test if inhibiting steady-state levels of endogenous EGFR alters *TERT* expression, we treated six GBM cell lines with three distinct EGFR inhibitors or separately with shRNAs targeting *EGFR*. Whether by pharmacologic or genetic means, reducing EGFR activity in cell lines with *TERT*_p mutation consistently decreased *TERT* expression, with a single exception (Lapatinib in SF7996, **Figure 3.3A**), an effect not seen in *TERT*_p wildtype lines (**Figure 3.2E, Figure 3.3A**). Furthermore, shRNA knockdown or pharmacologic inhibition of EGFR in an *EGFR* amplified patient-derived cell culture, GBM6, also significantly decreased *TERT* expression (**Figure 3.2E-F**). The exclusivity of these *TERT* responses to EGFR inhibition in cell lines with the *TERT*_p mutation suggests EGFR signaling specifically activates the mutant promoter. To test the specificity for the mutant *TERT*_p in an isogenic background, we compared the effect of EGFR inhibition on luciferase activity in LN229 cells with either the WT or mutant *TERT*_p driving luciferase. These experiments demonstrate that EGFR inhibition regulates the C228T and C250T mutant *TERT*_p, while not affecting activity of the WT promoter (**Figure 3.2G**). From these results, we conclude that EGFR activation selectively stimulates expression the mutant *TERT*_p in GBM cells.

The two most common *TERT*_p mutations, C228T and C250T create ETS transcription factor binding motifs that recruit the heterotetrameric form of the ETS factor GABP, selectively activating the mutant *TERT*_p (Huang et al 2013; Bell et al 2015; Mancini et al 2018). Given the specificity of EGFR signaling in regulating the mutant but not WT *TERT*_p (**Figure 3.2B-G**), we next sought to determine whether this regulation involved GABP. Using the same stratification of TCGA tumors into pEGFR-high and pEGFR-low groups (**Figure 3.2A**) we found that the average *GABPB1* expression was significantly elevated in EGFR-high tumors, and *GABPA* mRNA showed a trend towards being elevated (**Figure 3.5A-B**).

This statistically significant association between EGFR phosphorylation and GABP expression in tumor tissue (**Figure 3.5A-B**) led us to hypothesize that EGFR activation of the mutant *TERT*_p is mediated by transcriptional upregulation of one or more GABP subunits. To test this hypothesis, we measured *GABPA* and *GABPB1* after modulating EGFR signaling. Using the inducible EGFR_{vIII}, we found that EGFR_{vIII} rapidly increases *GABPB1* expression (**Figure 3.4A-B**). EGF stimulation in *TERT*_p mutant GBM cells also increased expression of both *GABPA* and *GABPB1* (**Figure 3.4C-D**). Conversely, shRNA-mediated knockdown of *EGFR* as well as pharmacologic inhibition of EGFR reduced *GABPA* and *GABPB1* expression (**Figure 3.4E-F, 3.3C-D**). Cumulatively these data connect EGFR signaling to GABP and EGFR to regulation of the mutant *TERT*_p.

We next asked whether EGFR regulates *TERT* expression through GABP. When we inhibited EGFR pharmacologically, the reduced GABP expression was accompanied by a decrease in GABP occupancy at the mutant *TERT*_p (**Figure 3.4G**). Furthermore,

transient knockdown of GABP expression reduced EGFRvIII-stimulated activity of the mutant *TERT*_p and reduced EGF-stimulated *TERT* expression (**Figure 3.4H-J**). In contrast, there was no change in activity of the wildtype *TERT*_p (**Figure 3.4I**). Together these results implicate EGFR signaling in the regulation of GABP subunit expression and subsequently *TERT* regulation via direct GABP binding to the mutant *TERT*_p.

Multiple pathways downstream of EGFR could play a role in EGFR regulation of GABP and *TERT*. One downstream mediator of EGFR signaling of special interest is AMPK, a heterotrimeric complex composed of α , β , and γ subunits that plays a key role in energy sensing and cellular metabolism. AMPK has been described as tumorigenic and tumor suppressing in tissue-specific contexts and in different cellular energy states (Ríos et al 2013; Faubert et al 2013; Shaw et al 2004; Inoki et al 2006; Jones et al 2005). Though AMPK has been most widely studied as a metabolic regulator, multiple studies report a new role as a stimulator of proliferation in glioma (Ríos et al 2013; Chhipa et al 2018). AMPK signaling is overactive in GBM compared to normal brain and drives tumorigenesis in part through transcriptional activation of *GABPA* (Chhipa et al 2018). AMPK regulates oncogenic signaling downstream of EGFR overexpression and EGF stimulation in other cancer contexts, suggesting AMPK as a potential link between EGFR and GABP regulation (Han et al 2018; Katreddy et al 2018). In RPPA data from GBM, the level of activating phosphorylation of threonine 172 on PRKAA1 (AMPKA1_PT172) (Stein et al 2000) is significantly higher in pEGFR-high tumors than pEGFR-low tumors, further supporting that EGFR signaling and AMPK signaling are associated in GBM (**Figure 3.5C**). To determine if the strong statistical association of EGFR-AMPK activity in patient tumor tissue reflects a functional relationship, we

stimulated cells with EGF or overexpressed EGFRvIII. With either approach to activate EGFR signaling, AMPK activation, as determined by phosphorylation of T172, was increased (**Figure 3.6A-D**).

With a firm connection established between EGFR signaling and AMPK activity in GBM tissue and across multiple cell lines, we turned our attention to the question of how AMPK signaling may in turn influence regulation of the mutant *TERT*_p. The *PRKAB1* subunit of the AMPK complex is overexpressed in GBM and is essential for kinase activity of AMPK and downstream signaling in GBM (Chhipa et al, 2018). Our analysis of TCGA RNA-Seq data demonstrated a strong correlation between expression of the AMPK subunit *PRKAB1* and both *GABPA* and *GABPB1* (**Figure 3.7A-B**).

Therefore, we took three independent approaches to determine if AMPK signaling regulates transcription of one or both GABP isoforms. First, we overexpressed dominant negative *PRKAA2*, which disrupts AMPK signaling (Chhipa et al, 2019), and observed that *GABPA* and *GABPB1* expression was reduced (**Figure 3.6E-F**). Second, we used shRNA knockdown of the AMPK regulatory subunit *PRKAB1*, which also reduced *GABPA* and *GABPB1* mRNA and protein (**Figure 3.6G-I**). Third, we generated full gene knockouts of *PRKAB1* using guides flanking the entire mRNA-coding portion of the gene. Three independent full gene knock out clones were validated by PCR and sequencing from genomic DNA and lacked detectable *PRKAB1* mRNA and protein. *TERT* mRNA expression and telomerase activity, as well as *GABPA* and *GABPB1* mRNA and protein expression were all consistently reduced in the three knock out clones (**Figure 3.8A-D**). Given the consistent results of these orthogonal approaches, we concluded that AMPK positively regulates *GABPA* and *GABPB1*.

The AMPK-mediated increase in GABP subunit expression could potentially drive increased *TERT* expression. Therefore, we next measured *TERT* expression, *TERT*_p activity, and GABP occupancy of the mutant *TERT*_p following AMPK modulation. Along these lines, overexpression of dominant-negative PRKAA2 decreased *TERT* expression (**Figure 3.9A**). Similarly, knockdown of *PRKAB1* reduced *TERT* expression, reduced promoter activity in a mutation-specific manner, and decreased binding of GABP to the mutant *TERT*_p (**Figure 3.9B-D**). We further asked if EGFR's upregulation of *TERT* (**Figure 3.2B-C**) is dependent on AMPK. We stimulated *PRKAB1* KO cells with EGF and observed no stimulatory effect on *TERT* (**Figure 3.8E**) compared to the significant stimulation of *TERT* expression in parental. AMPK signaling therefore regulates the mutant *TERT*_p through GABP subunit modulation.

The elevated *TERT* expression downstream of EGFR-AMPK signaling may have little functional consequence, or alternatively, it could provide the increased telomerase activity required for telomere maintenance in the rapidly dividing GBM cells. To distinguish between these possibilities, we first knocked down *PRKAB1* and *EGFR* and measured telomerase activity. Either *PRKAB1* or *EGFR* knockdown was sufficient to reduce telomerase activity in *TERT*_p mutant, but not *TERT*_p WT GBM cells (**Figure 3.10A-B**). In addition to reduced telomerase activity, proliferation slowed slightly in the *EGFR* and *PRKAB1* knockdown cells, consistent with the canonical roles of EGFR and AMPK in pro-growth signaling (**Figure 3.11**). Telomerase activity lengthens telomeres while rapid cell division shortens them. As our data and prior studies suggest, EGFR-AMPK can regulate both of these central cancer cell phenotypes. We asked whether knockdown of *PRKAB1* or *EGFR* would lead to telomere attrition in cells that are still

actively dividing, albeit with a slight reduction (**Figure 3.11**). Following the cells over a 40-60 day period, we observed progressive telomere shortening in *TERT*_p mutant GBM cells with *EGFR* or *PRKAB1* knockdown, but not in *TERT*_p wildtype cells (**Figure 3.10C-D**). The telomere shortening could be rescued in *PRKAB1* and in *EGFR* knockdown cells by re-expression of ectopic *TERT* (**Figure 3.10E-F**). We conclude that reduced telomerase activity caused by *EGFR* and *PRKAB1* knockdown in actively dividing GBM cells leads to telomere attrition.

Using a converse approach to knockdown, we asked whether the increased *TERT* expression from EGFR activation is functionally important in telomere maintenance. Knocking down *TERT* alone resulted in telomere shortening over time (Figure 7A). In the context of *TERT* knockdown and EGFRvIII overexpression however, *TERT* expression increased. This moderate increase in *TERT* by EGFRvIII, despite the continued presence of the *TERT* shRNA, was sufficient to maintain the telomeres at a longer length than in *TERT* shRNA only cells (**Figure 3.12A-B**), though slightly shorter in length compared to parental controls. This suggests that the lower level of *TERT* expression in the *TERT* knockdown cells may not be sufficient to maintain telomere length, whereas the increased *TERT* expression by EGFR signaling contributes to maintaining telomere length. Collectively, we posit a model by which EGFR-AMPK signaling regulates the mutant *TERT*_p through modulation of GABP expression and GABP occupancy at the mutant *TERT*_p, and consequently attenuates telomere erosion caused by cell division (**Figure 3.12C**).

Discussion

This is the first study directly linking EGFR to mutant *TERT*_p regulation in any type of cancer. A previous study in epidermoid carcinoma linked EGFR to *TERT* expression in *TERT*_p wildtype cells through activation of the MAPK pathway (Maida et al 2002). This suggests there may be regulation of TERT that is unique to the mutant versus wildtype *TERT*_p. Our studies did not observe an effect of EGFR on *TERT*_p wildtype GBM cells, which could also suggest cancer type specific regulation of the wildtype *TERT*_p by EGFR. To our knowledge, GBM is the only cancer with a co-occurrence of EGFR activation and *TERT*_p mutation. MAPK signaling has also been linked to mutant *TERT*_p regulation in six cancer cell lines (Li et al 2016). Future studies could explore if MAPK links EGFR to *TERT* regulation in GBM.

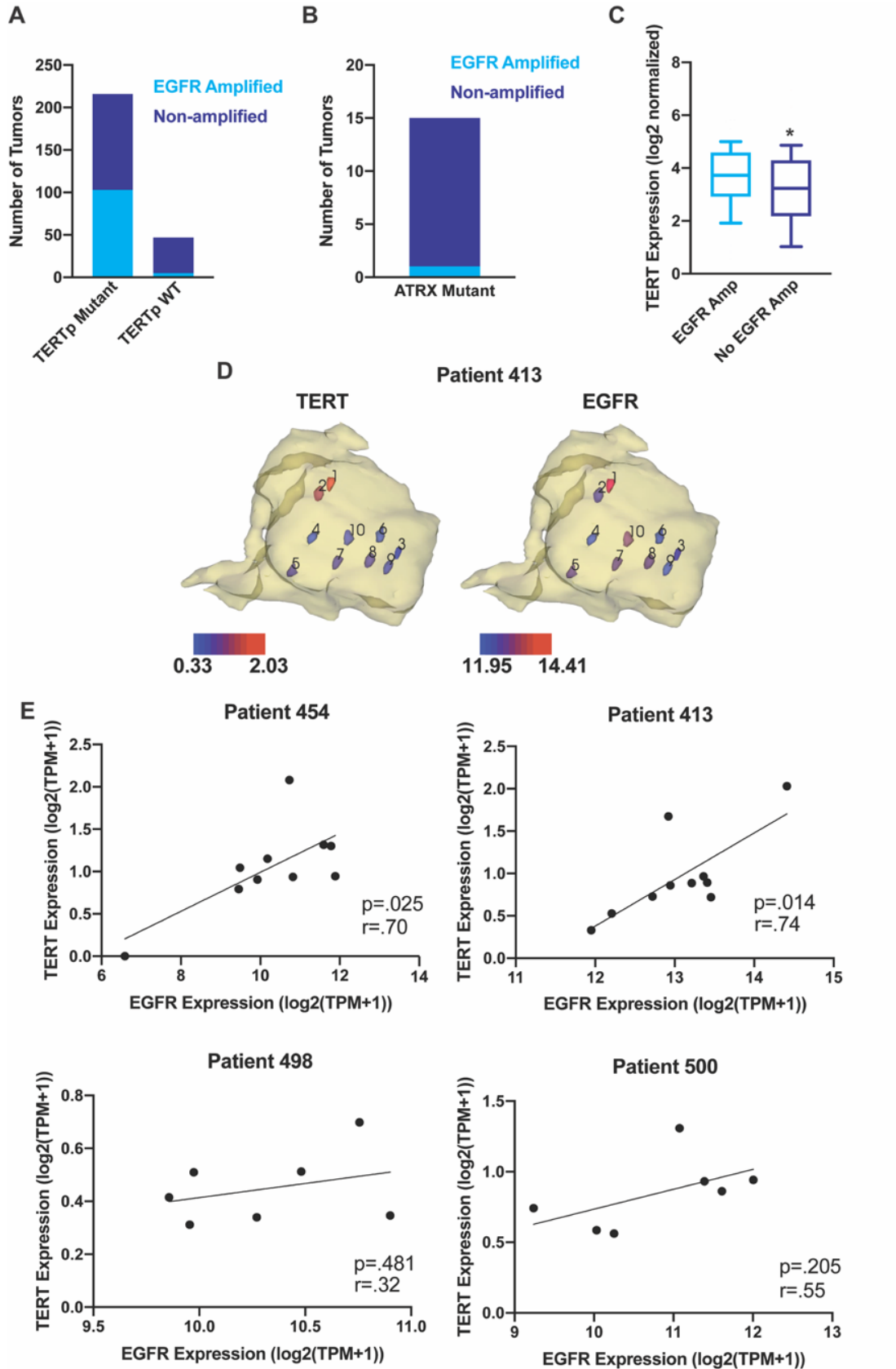


Figure 3.1 *TERT* expression correlates with *EGFR* amplification and *EGFR* expression in human GBM

(A) Number of *IDH1*-WT GBM tumors harboring *EGFR* amplification in *TERT*_p mutant or *TERT*_p-WT tumors in MSK-IMPACT data. Fisher exact probability test, two tailed, $p < 0.0001$. (B) Number of *IDH1*-WT GBM tumors harboring *EGFR* amplification in *ATRX* mutant cancers in MSK-IMPACT data. (C) *TERT* mRNA expression in *EGFR* amplified or non-amplified *IDH1*-WT GBM tumors (TCGA data). Tumors with available RNA-Seq data and tumor purity greater than 60% were stratified into 61 *EGFR* amplified and 46 non-amplified cases. Whiskers represent 5th and 95th percentile values. Wilcoxon rank-sum test, two-tailed. * $P < 0.05$. (D) log₂-normalized mRNA expression from 10 intratumoral, spatially mapped samples for *TERT* (left) and *EGFR* (right) in the 3D context of the tumor (yellow, tumor derived from T2 MRI) (E) Correlation of log₂-normalized relative *EGFR* and *TERT* expression within 7-10 intratumoral samples (tumor purity of each sample is greater than 60%) from each of three *EGFR* amplified GBM tumors. r represents Pearson correlation coefficient

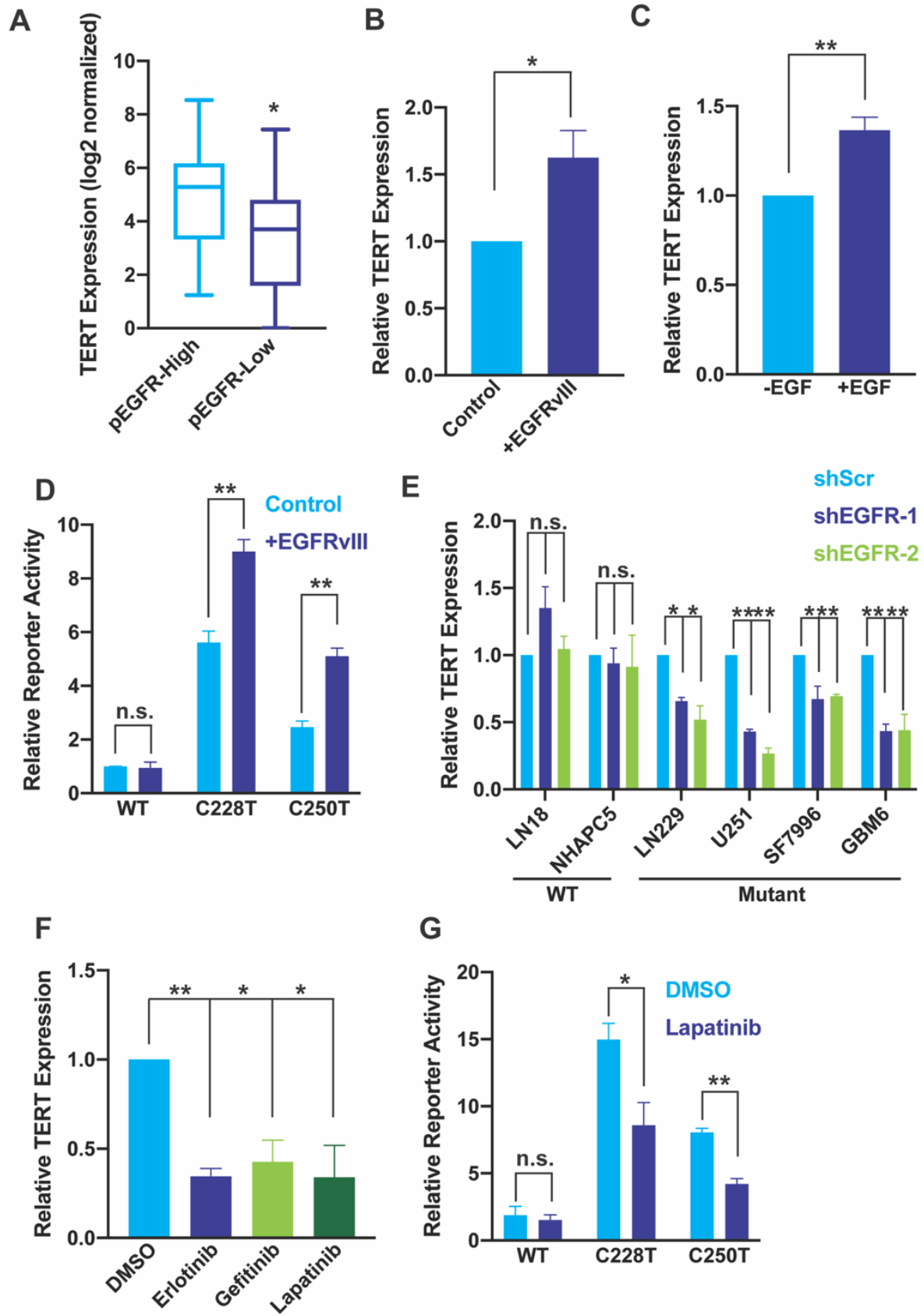


Figure 3.2 EGFR signaling selectively upregulates the mutant *TERTp*

(A) *TERT* mRNA expression in *IDH1*-WT GBMs with different EGFR expression. Tumors profiled by TCGA with available RNA-Seq and RPPA data, and tumor purity greater than 60%, were stratified into 27 EGFR-high, 27 EGFR-low cases by RPPA expression. Whiskers represent 5th and 95th percentile values. Wilcoxon rank-sum test, two-tailed * $P < 0.05$, ** $P < .005$. (B) *TERT* expression measured by RT-qPCR after 12 hours doxycycline induction of EGFRvIII in serum starved U251 cells. Data are normalized relative to serum starved cells (-doxycycline) within each replicate. (C) *TERT* expression measured by RT-qPCR after 12 hours EGF induction in serum starved U251 cells. Data are normalized relative to the serum starved (-EGF) condition within each replicate. (D) *TERTp*-luciferase reporter assays after 12 hours of EGFRvIII induction in serum starved U251 cells. Data are normalized relative to WT reporter activity in serum starved cells (-EGFRvIII induction) within each replicate. (E) *TERT* expression after 72 hours of shRNA targeting EGFR, measured by RT-qPCR in LN18, NHAPC5, LN229, U251, SF7996, and GBM6 cells. Data are normalized relative to scrambled control (shScr) for each cell line. (F) *TERT* expression after 72 hours of treatment of GBM6 cells with 1 μ M EGFR inhibitor, measured by RT-qPCR. Data are normalized relative to DMSO within each replicate. (G) *TERTp*-luciferase reporter assays in LN229 cells after 72 hours of pharmacological EGFR inhibition. Data are normalized relative to DMSO treated WT reporter. (B-G), Student's t-tests, two-tailed. * $P < 0.05$, ** $P < .005$, data represent mean \pm SEM

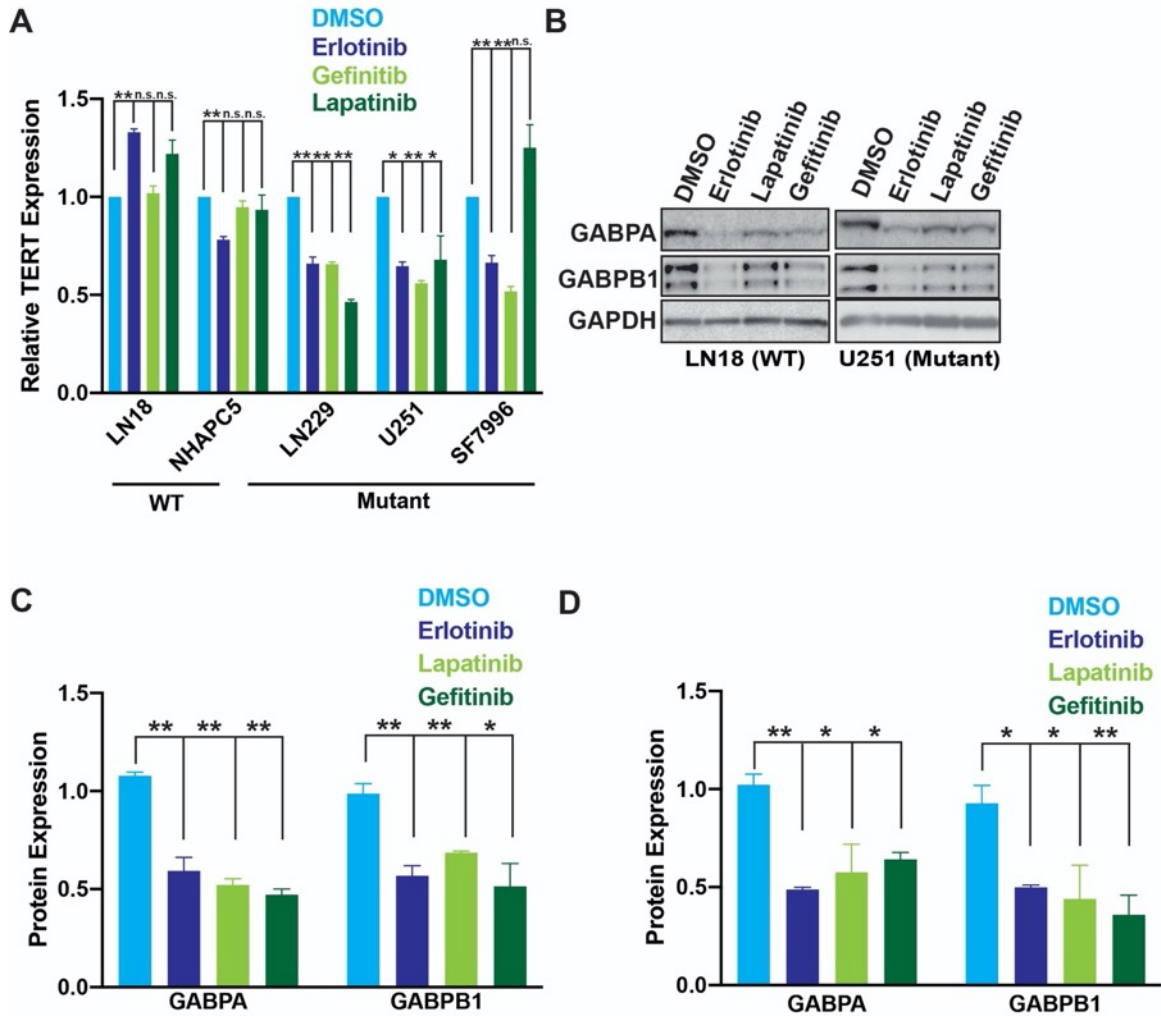


Figure 3.3 Pharmacological inhibition of EGFR downregulates the GABP-TERT axis

(A) *TERT* expression upon pharmacological EGFR inhibition (5uM for all three inhibitors) measured by RT-qPCR, normalized relative to DMSO in each cell line. (B) Representative immunoblots of GABPA and GABPB1 upon pharmacological EGFR inhibition compared to DMSO (leftmost lane). (C-D) Quantification of LN18 (C) and U251 (D) immunoblots of GABP subunits from panel B.

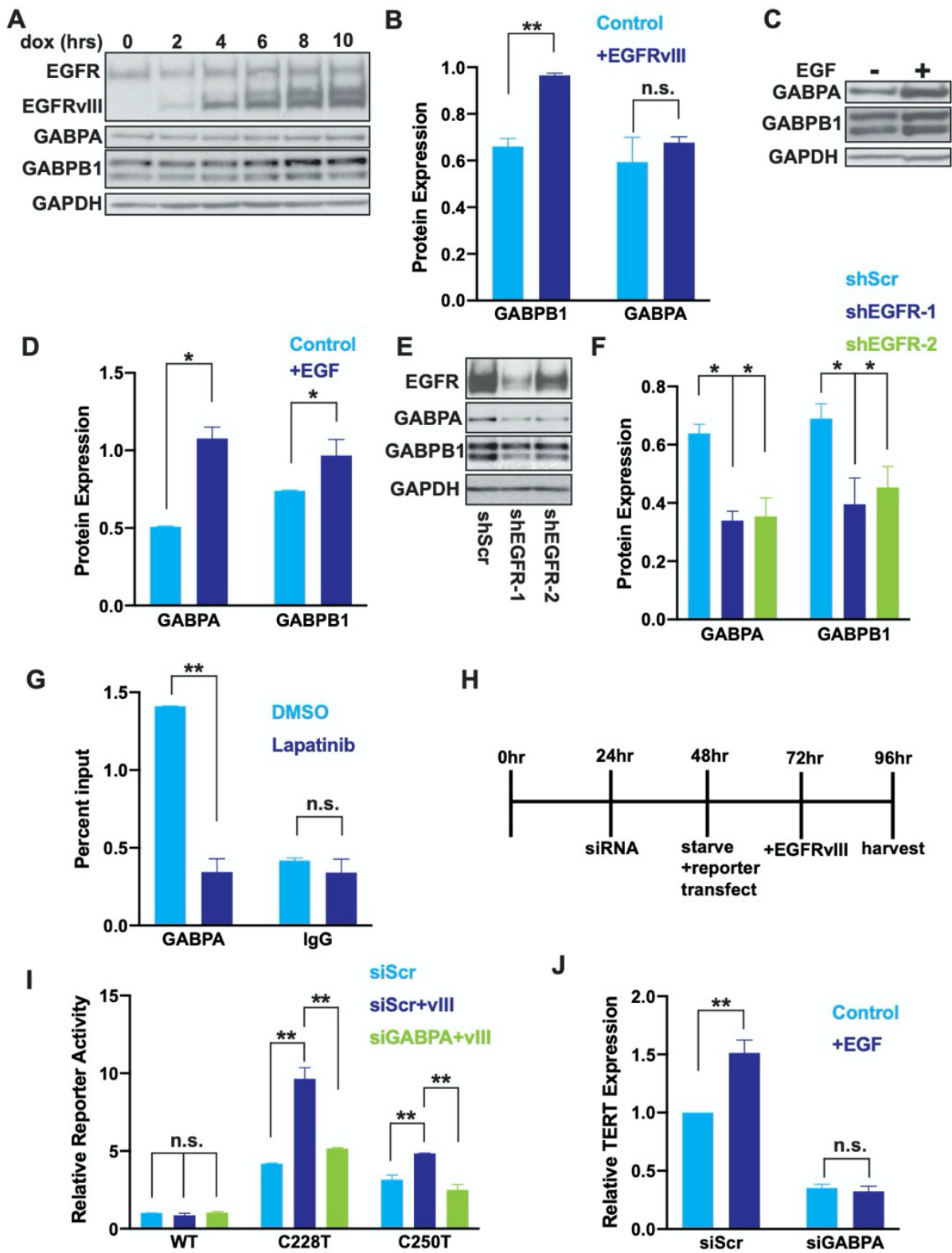


Figure 3.4 EGFR signaling upregulates the mutant *TERT*_p by increasing GABP expression

(A) Representative immunoblots of EGFR, GABPA and GABPB1 after induction of EGFR^{vIII} expression in U251 cells. (B) Quantification of the 10-hour timepoint of immunoblots from panel A. (C) Immunoblots of GABPA and GABPB1 after 12 hours of EGF induction in serum starved LN229 cells. (D) Quantification of immunoblots from panel C. (E) Immunoblots of EGFR, GABPA, and GABPB1 after 72 hours of shRNA targeting EGFR in LN229 cells. (F) Quantification of immunoblots from panel E. (G) GABPA and IgG isotype control ChIP-qPCR for the *TERT*_p after 72 hours pharmacological EGFR inhibition in LN229 cells. (H) Experimental timeline of EGFR^{vIII} induction and luciferase reporter assay after serum starvation, for data in panel I and J. (I) *TERT*_p-luciferase reporter activity in U251 cells treated for 72 hours with siRNAs targeting *GABPA* or scrambled control (siScr). Data are normalized relative to serum starved U251 cells with siScr, WT reporter activity within each replicate. (J) *TERT* expression measured by RT-qPCR following a 12 hour EGF induction in serum starved cells that were also treated with siRNAs for 72 hours targeting *GABPA* or siScr control in LN229 cells. Data are normalized relative to serum starved cells (-EGF) within each condition. (B-G, I-J) Student's t-tests, two-tailed. *P<0.05, **P<.005, data represent mean +/- SEM.

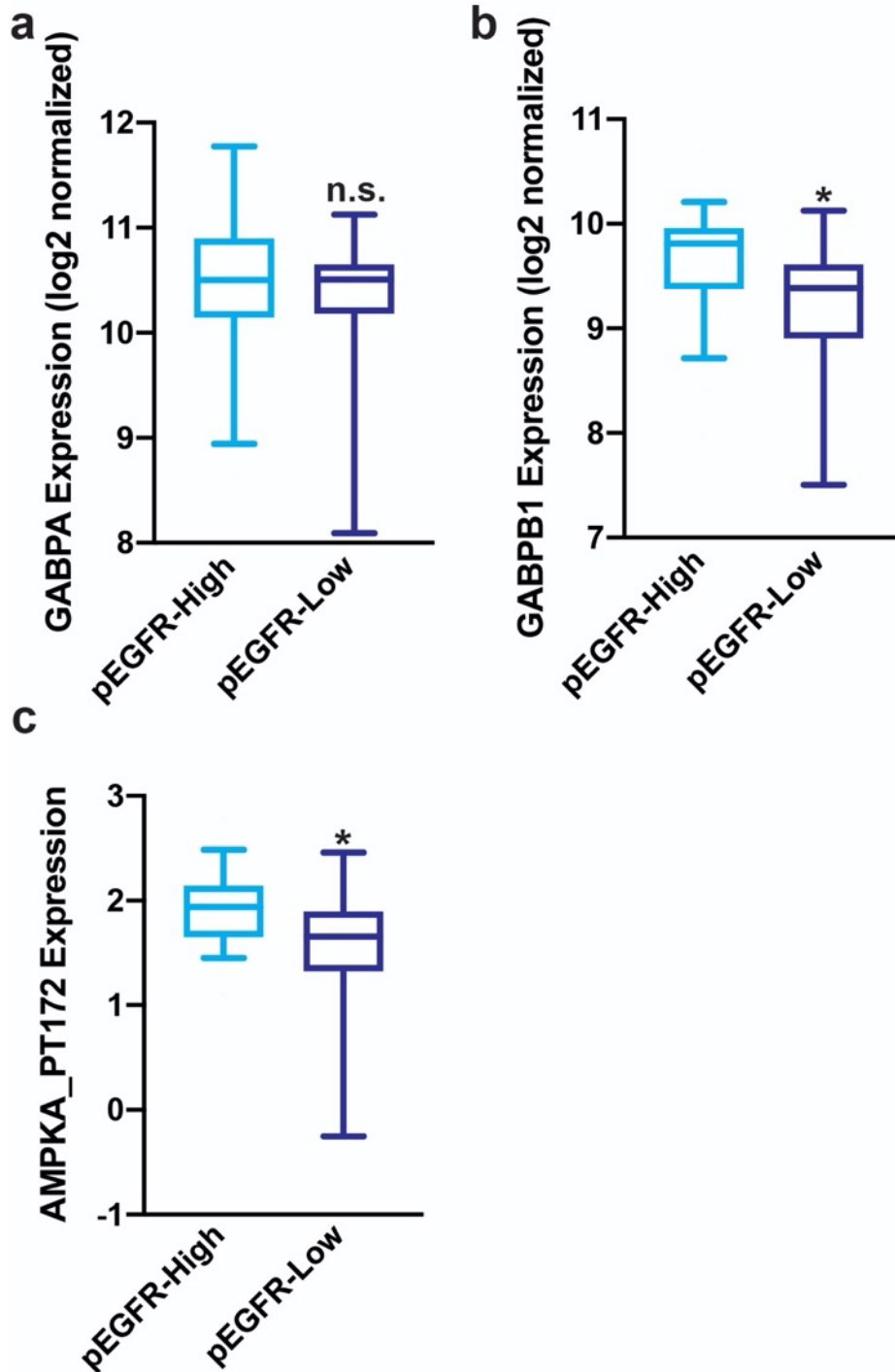


Figure 3.5 GABP and p-AMPK are elevated in EGFR-high GBM

(A) *GABPA* mRNA expression in *IDH1*-WT GBM tumors. Tumors profiled by TCGA with available RNA-Seq and RPPA data were stratified into 27 EGFR-high, 27 EGFR-low. Whiskers represent 5th and 95th percentile values. Samples with less than 60% purity

were excluded. (B) *GABPB1* mRNA expression in *IDH1*-WT GBM tumors. Tumors profiled by TCGA with available RNA-Seq and RPPA data were stratified into 27 EGFR-high, 27 EGFR-low. Whiskers represent 5th and 95th percentile values. Samples with less than 60% tumor purity were excluded. (C) Expression of endogenous AMPKA1_PT172 in EGFR amplified or non-amplified *IDH1*-WT GBMs. Tumors profiled by TCGA with available RNA-Seq and RPPA data and tumor purity greater than 60%, were stratified into 27 EGFR-high, 27 EGFR-low cases. Whiskers represent 5th and 95th percentile values. (A-C) Wilcoxon rank-sum test, two-tailed. * $P < 0.05$.

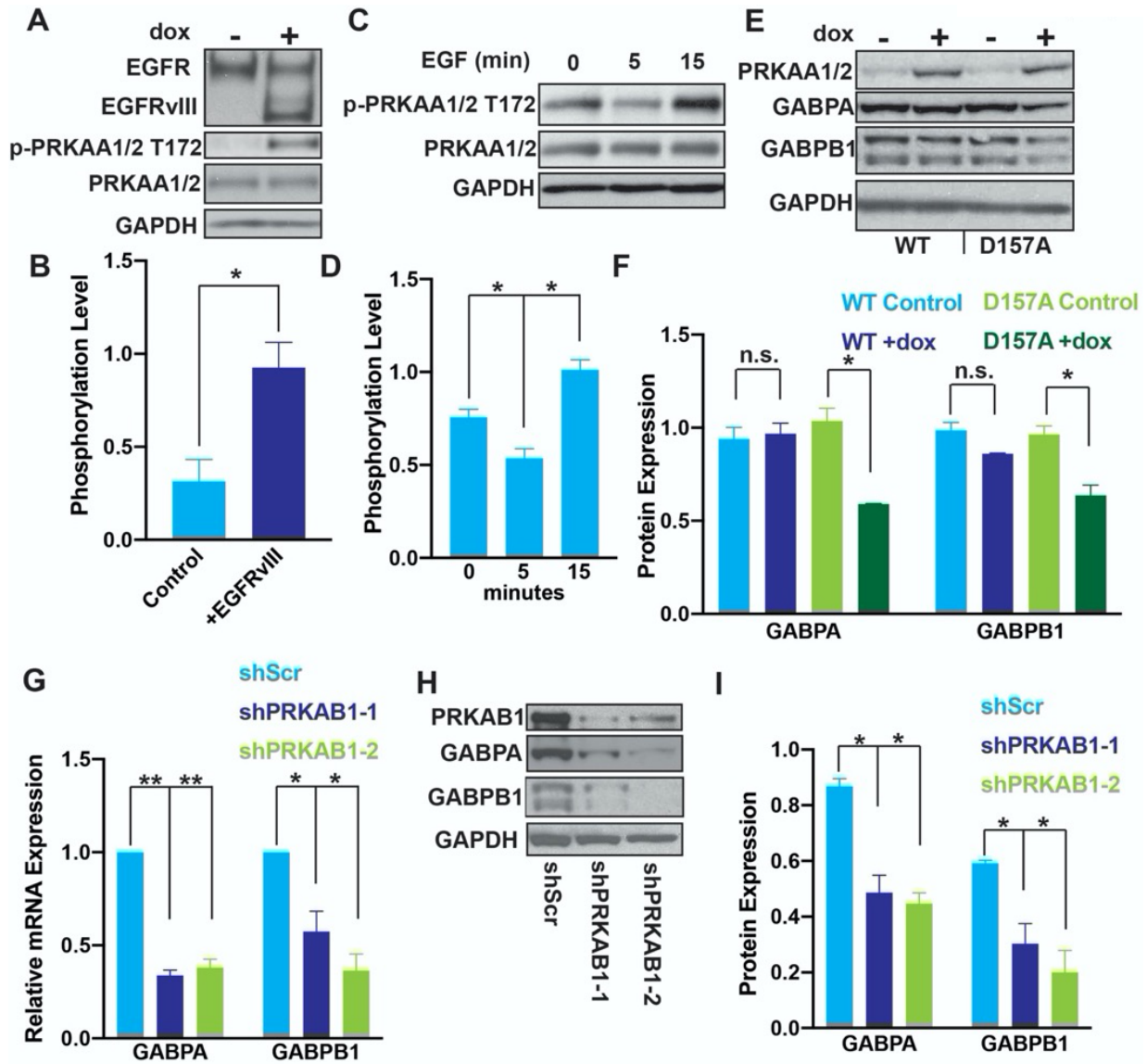


Figure 3.6 Activated AMPK upregulates GABP subunit expression downstream of EGFR

(A) Representative immunoblots of EGFR, p-PRKAA1/2 T172 and PRKAA1/2 after doxycycline induction of EGFRvIII in U251 cells. (B) Quantification of immunoblots from panel A. Data are expressed as ratio of p-PRKAA1/2 to total PRKAA1/2 within each replicate. (C) Representative immunoblots of p-PRKAA1/2 T172 and PRKAA1/2 upon EGF induction in serum starved LN229 cells. (D) Quantification of immunoblots from panel C. Data are expressed as the ratio of p-PRKAA1/2 to total PRKAA1/2 within each replicate. (E) Representative immunoblots of PRKAA1/2, GABPA, and GABPB1 upon doxycycline-induction of PRKAA1/2 (WT) or catalytically-dead PRKAA1/2 (D157A) expression in LN229 cells. (F) Quantification of immunoblots from panel E. (G) *GABPA*

and *GABPB1* mRNA expression upon shRNA-mediated knockdown of *PRKAB1* in LN229 cells, measured by RT-qPCR. (H) Immunoblots of GABPA, GABPB1, and PRKAB1 after 72 hours shRNA-mediated *PRKAB1* knockdown in LN229 cells. (I) Quantification of immunoblots from panel H. (A-I) Student's t-tests, two-tailed. *P<0.05, **P<.005, data represent mean +/- SEM.

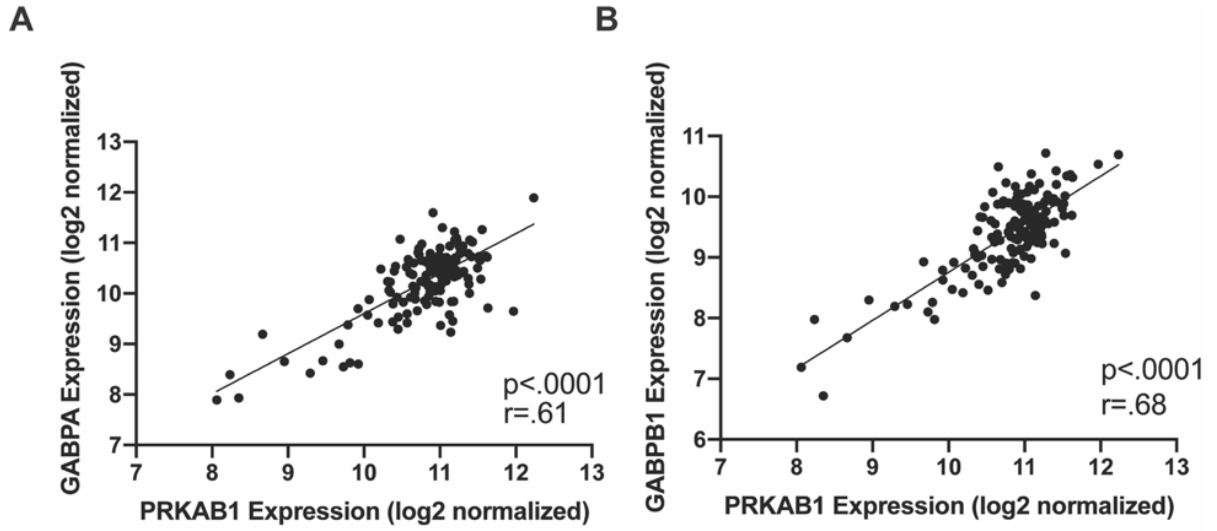


Figure 3.7 *PRKAB1* correlates with GABP subunit expression in GBM

(A-B) Correlation of log2 RNA-Seq of GBMs from TCGA of *PRKAB1* with *GABPA* (A) and *GABPB1* (B). r, Pearson coefficient, $p < .0001$

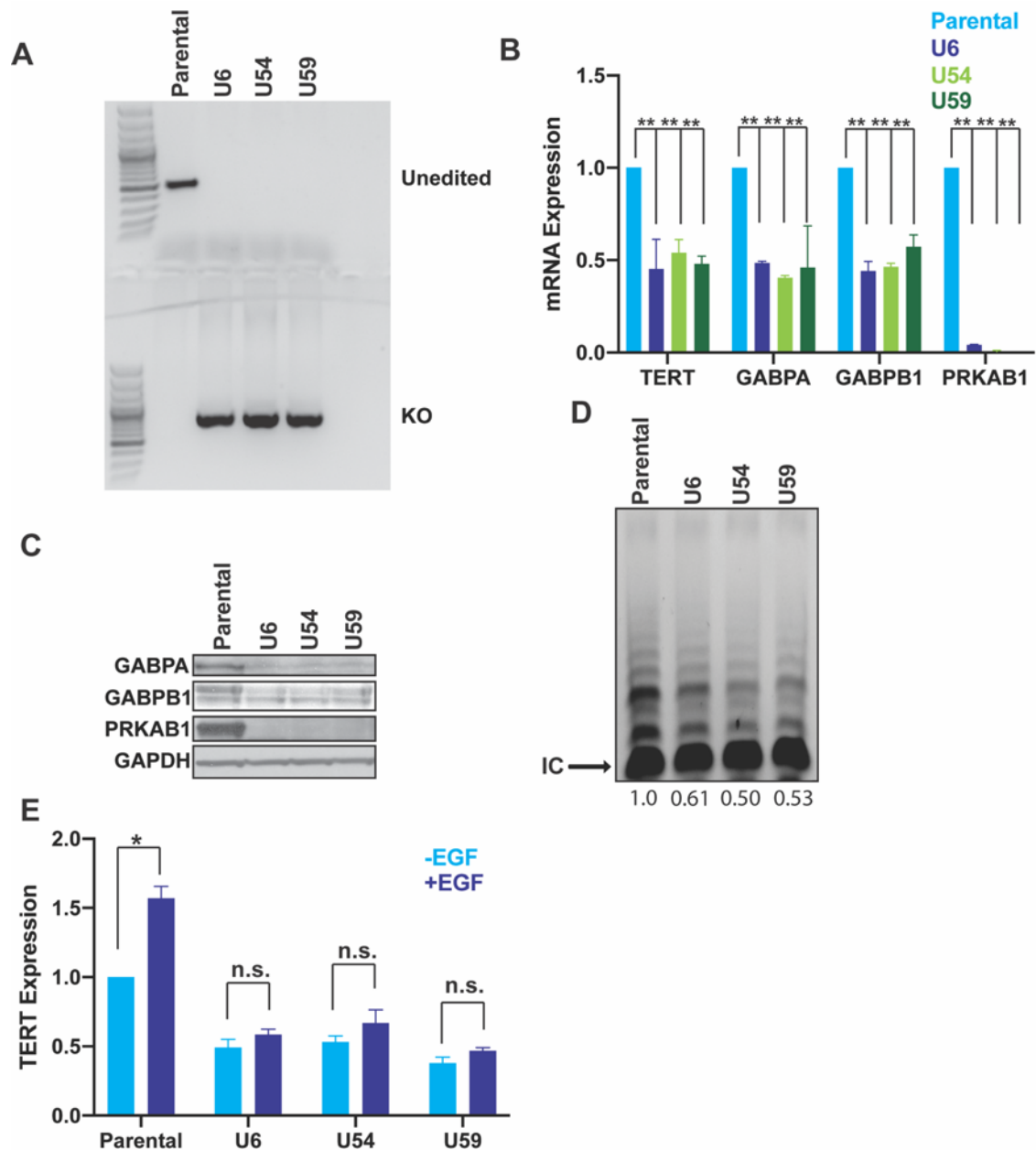


Figure 3.8 CRISPR-mediated full gene knockout of *PRKAB1* reduces GABP and *TERT*

(A) Genotyping analysis of *PRKAB1* full gene knockout clones (U6, U54, and U59) compared to parental U251 cells. (B) mRNA levels of *TERT*, *GABPA*, *GABPB1* and *PRKAB1* in U251 *PRKAB1* full gene knockout clones measured by RT-qPCR, relative to parental, unedited U251 cells. Student's t-tests. ** $P < .005$, data represent mean \pm SEM. (C) Immunoblots of *GABPA*, *GABPB1*, and *PRKAB1* in U251 *PRKAB1* total knockout clones. (D) Telomerase activity of U251 *PRKAB1* total knockout clones. (E) *TERT* expression measured by RT-qPCR following a 12 hour EGF induction in serum

starved cells in full knockout clones (U6, U54, U59) compared to parental U251 cells. Student's t-tests. *P<0.05, data represent mean +/- SEM.

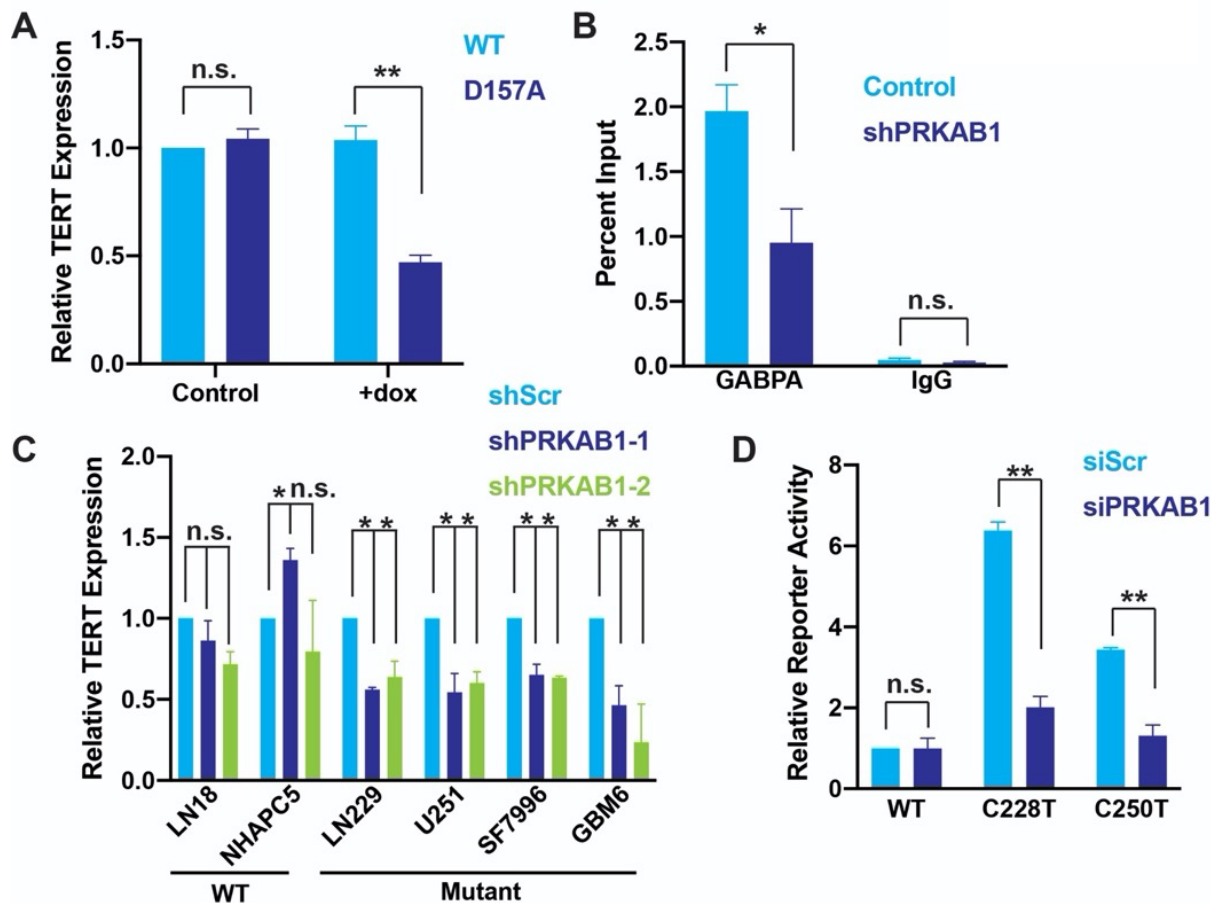


Figure 3.9 AMPK signaling selectively regulates the mutant *TERT*_p

(A) GABPA ChIP-qPCR for the *TERT*_p after 72 hour doxycycline-inducible shRNA-mediated *PRKAB1* knockdown in LN229 cells. IgG isotype was used as a control. Data are expressed as a percentage of genomic DNA input. (B) *TERT* expression measured by RT-qPCR after 72-hour doxycycline-induction of *PRKAA2* (WT) or catalytically-dead *PRKAA2* (D157A) expression in LN229 cells. Data are normalized relative to uninduced WT *PRKAA2*-vector containing cells within each replicate. (C) *TERT* expression upon shRNA-mediated knockdown of *PRKAB1* measured by RT-qPCR in LN18, NHAPC5, LN229, U251, SF7996, and GBM6 cell lines and patient-derived cultures. Data are normalized relative to shScr control. (D) *TERT*_p-luciferase reporter assays after 72-hour siRNA-mediated knockdown of *PRKAB1* for WT, C228T and C250T promoters. Data are normalized relative to siRNA scramble control *TERT*_p WT reporter in LN229 cells. (A-D) Student's t-tests, two-tailed. * $P < 0.05$, ** $P < 0.005$, data represent mean \pm SEM

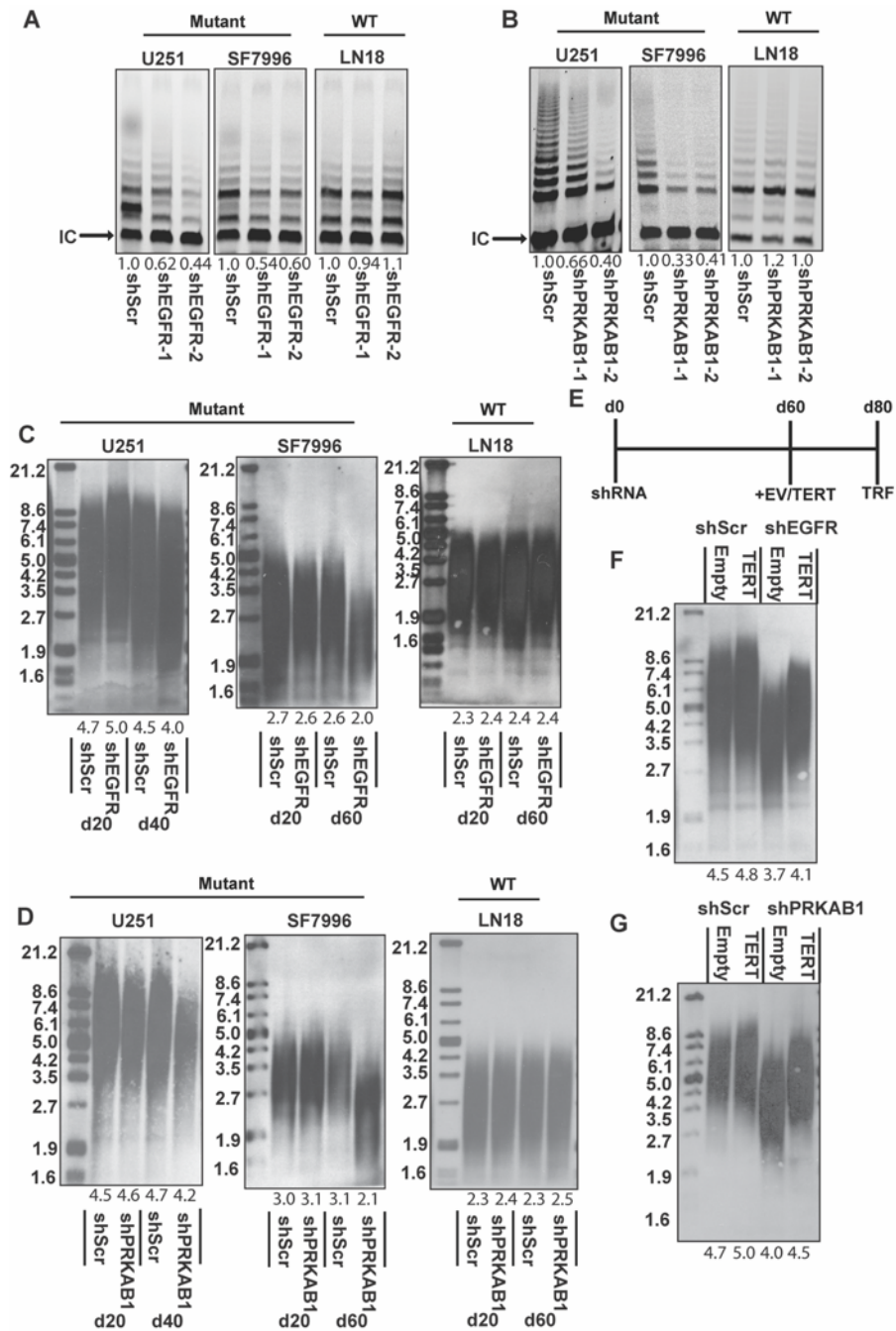


Figure 3.10 The EGFR-AMPK axis regulates telomerase activity and telomere length in *TERT*p mutant GBM

(A) Telomerase activity after 6 days of shRNA-mediated knockdown of EGFR normalized to internal control band (IC). (B) Telomerase activity after 6 days of shRNA-mediated knockdown of PRKAB1 normalized to internal control band (IC). (C) Telomere length assessed by telomere restriction fragmentation after shRNA-mediated knockdown of PRKAB1 in U251, SF7996, and LN18 cells. (D) Telomere length

assessed by telomere restriction fragmentation after shRNA-mediated knockdown of PRKAB1 in U251, SF7996, and LN18 cells. (E) Timeline of long-term telomere restriction fragmentation *TERT* rescue experiments (F) Telomere length assessed by telomere restriction fragmentation after shRNA-mediated knockdown of EGFR in U251 followed by rescue with *TERT* coding sequence or empty vector. (G) Telomere length assessed by telomere restriction fragmentation after shRNA-mediated knockdown of PRKAB1 in U251 followed by rescue with *TERT* relative to empty vector control.

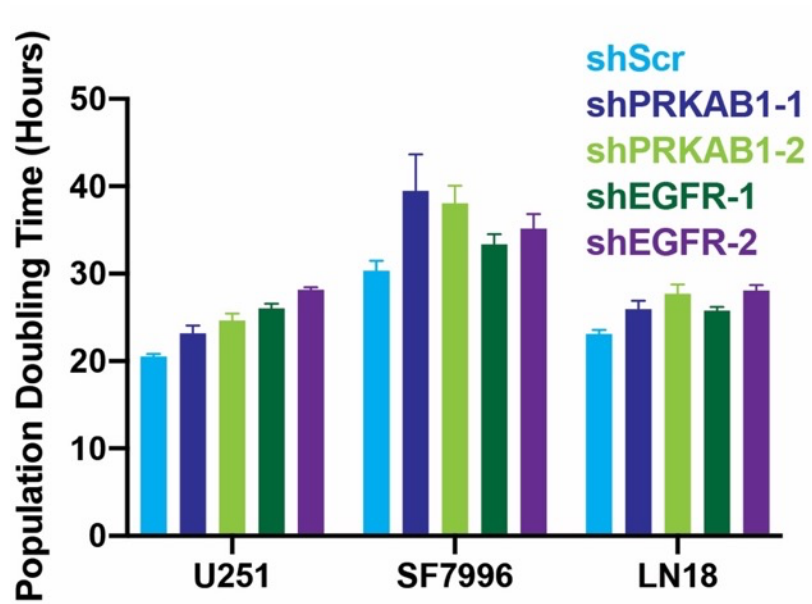


Figure 3.11 *EGFR* or *PRKAB1* inhibition slows cell doubling time

Population doubling time upon shRNAs knockdown of *PRKAB1* or *EGFR*.

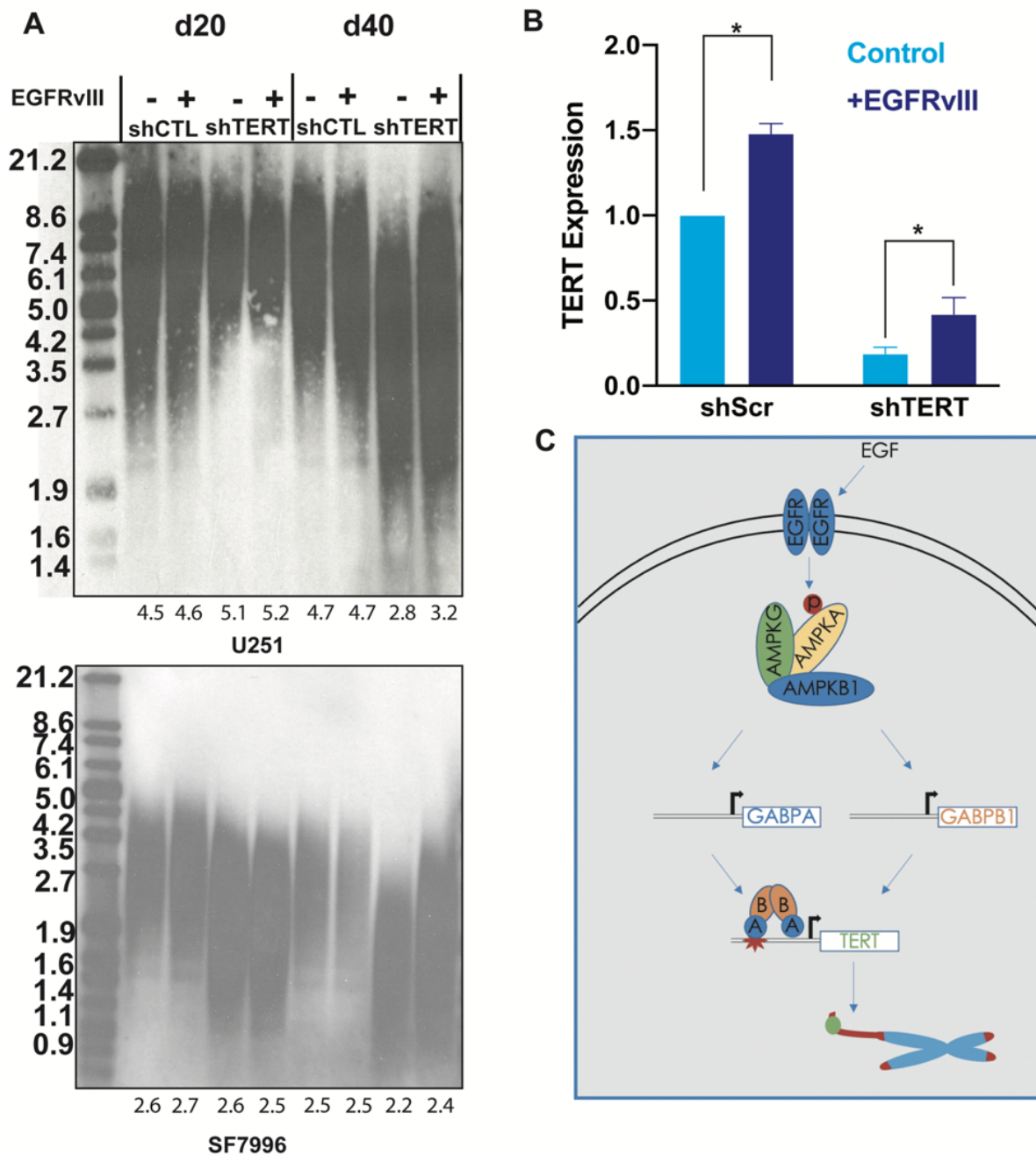


Figure 3.12 *EGFR* overexpression counteracts telomere shortening from *TERT* knockdown

(A) Telomere length assessed by telomere restriction fragmentation after shRNA-mediated *TERT* knockdown and doxycycline induction of EGFRvIII in U251 (top panel) and SF7996 (bottom panel) cells, (B) *TERT* expression measured by RT-qPCR after shRNA-mediated *TERT* knockdown and doxycycline induction of EGFRvIII in U251 cells

at the 40-day timepoint. Student's t-tests, two-tailed. * $P < 0.05$, data represent mean \pm SEM. (C) Model of EGFR-AMPK regulation of the mutant *TERT*_p via GABP.

**CHAPTER 4: CIC INACTIVATION STIMULATES THE *TERT*
PROMOTER IN OLIGODENDROGLIOMA**

Introduction

The two most common classes of lower grade glioma, astrocytoma and oligodendroglioma, differ in their mode of telomere maintenance. Astrocytoma utilize alternative lengthening of telomeres (ALT), usually via inactivation of the chromatin remodeling gene *ATRX*. Oligodendroglioma, like GBM, rely on telomerase via *TERTp* mutations in over 80% of cases. Unlike GBM, oligodendroglioma do not typically harbor *EGFR* amplification, leaving an open question which if any drivers of proliferation regulate *TERT* in oligodendroglioma.

CIC mutations occur in roughly 70-80% of oligodendroglioma (Sahm et al, 2012). *CIC* is a repressive transcription factor downstream of receptor tyrosine kinase signaling that = represses transcription of the ETS variant transcription factor (ETV) family of genes (Bunda et al, 2019). Inactivating mutations of *CIC* occur most predominantly at amino acid position 215 in the HMG box, which facilitates DNA binding, while a smaller subset occur in the protein binding region (Chittaranjan et al 2014). Additionally, an inverse correlation between *CIC* and cell proliferation has been reported in human glioma (Bunda et al, 2019), which may in part be related to *CIC* being repressed by receptor tyrosine kinase signaling which promotes cell proliferation. Therefore, I hypothesized that *CIC* mutations link cell proliferation and mutant *TERTp* regulation in oligodendroglioma.

Results

To determine if *CIC* regulates the mutant *TERTp*, we first determined if *CIC* mutations are associated with higher *TERT* expression in oligodendroglioma tumor tissue. Using a TCGA cohort of 26 *CIC* wild type and 26 *CIC* mutant tumors, we

observed that *TERT* expression was significantly higher in the mutant tumors (**Figure 4.1A**). Additionally, several ETS factors exhibited increased expression in *CIC* mutant tumors (**Figure 4.1B**). Knockdown of *CIC* by siRNA in *CIC* wild type GBM and oligodendroglioma patient-derived lines, SF7996 and SF10417, exhibited a significant increase in *TERT* expression, definitively linking *CIC* repression to mutant *TERT*_p activation (**Figure 4.2A**).

Eleven of 29 ETS factors are expressed in glioma (Bell, et al 2015). We screened mRNA expression of these eleven ETS factors in our oligodendroglioma cell line SF10417 after *CIC* knockdown and observed that two factors, *ETS1* and *ETV3*, were significantly upregulated, while one, *ELF1*, was significantly downregulated (**Figure 4.2B**). Neither the *GABPA* nor *GABPB1L* subunit that are responsible for mutant *TERT*_p activation were altered. Interestingly, previous work from our lab included an siRNA screen of ETS factors to test their effect on *TERT* regulation and demonstrated that knockdown of *ETS1*, *ETV3*, and *GABPA* all had a significant effect on *TERT* expression across two GBM cell lines, though *GABPA* was by far the most pronounced effect (Bell et al, 2015). *ELF1* is also of interest as it has been suggested recently as being an antagonist to *GABP* at the *TERT*_p. This suggests the possibility that *CIC* could regulate the mutant *TERT*_p through alternate ETS factors. To test this possibility, we performed combinatorial knockdowns of *CIC* in concert with siRNA targeting *ETS1*, *ETV3*, and *GABPA*. Even in the context of *GABPA* knockdown, *CIC* inhibition increased *TERT* expression. However, in the context of either *ETS1* or *ETV3* knockdown (**Figure 4.2C**), *CIC* no longer upregulated *TERT* expression, suggesting *CIC*'s repressive action on the mutant *TERT*_p is mediated by *ETS1* and *ETV3* upregulation, and not through *GABPA*.

Additionally, using a luciferase reporter assay, we observed that the wildtype *TERT*_p is upregulated by *CIC* knockdown, proving that this is not a mutant-specific phenomenon (Figure 4.2D).

Discussion

Here we observe that *CIC* can regulate *TERT* via transcription factors other than GABPA. This is consistent with previous reports of ETS factors other than GABP regulating the *TERT*_p to a lesser degree (Bell et al, 2015). It is known that GABP regulates the mutant *TERT*_p (Mancini et al, 2018). That other ETS factors can upregulate *TERT* suggests that in these cells GABP is not fully maximizing the activation potential of the mutant *TERT*_p in this cell context. Another explanation is that these ETS factors act on *TERT* via an indirect mechanism, or binding at a separate ETS site in the *TERT*_p outside of the mutant site. Additional experiments would be needed to directly show binding of ETS1 and ETV3 to the mutant *TERT*_p, either at the mutant site or elsewhere.

CIC is not the only potential oncogenic driver in oligodendroglioma that could regulate the mutant *TERT*_p. Further studies could explore the role of other common oncogenic drivers such as tumor suppressors in the 1p chromosome arm that is deleted in oligodendroglioma, or *FUBP1* mutations. *CIC* is also inactivated downstream of EGFR activation which could link the two pathways described in GBM and oligodendroglioma (Bunda et al, 2019), however the mutant-specific mechanism of EGFR is inconsistent with the described mechanism of *CIC*. *CIC* mutations are not currently druggable, so elucidating the pathway downstream of *CIC* would be necessary to therapeutically target the *TERT*_p in the *CIC* mutant context.

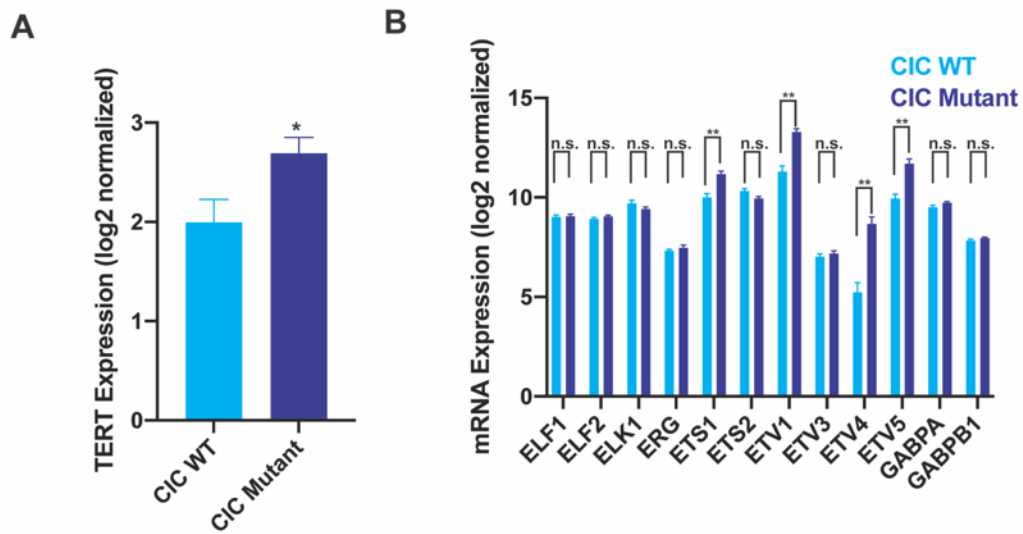


Figure 4.1 CIC mutant tumors express higher *TERT* and ETS factors

(A) *TERT* mRNA expression in *CIC* wild type (WT) or *CIC* mutant tumors. Tumors profiled by TCGA with available RNA-Seq and exome data, and tumor purity greater than 60% were used. Error bars represent SEM. Wilcoxon rank-sum test, two-tailed * $P < 0.05$, ** $P < .005$. (B) ETS factor mRNA expression in *CIC* wild type (WT) or *CIC* mutant tumors. Tumors profiled by TCGA with available RNA-Seq and exome data, and tumor purity greater than 60% were used. Error bars represent SEM. Wilcoxon rank-sum test, two-tailed * $P < 0.05$, ** $P < .005$.

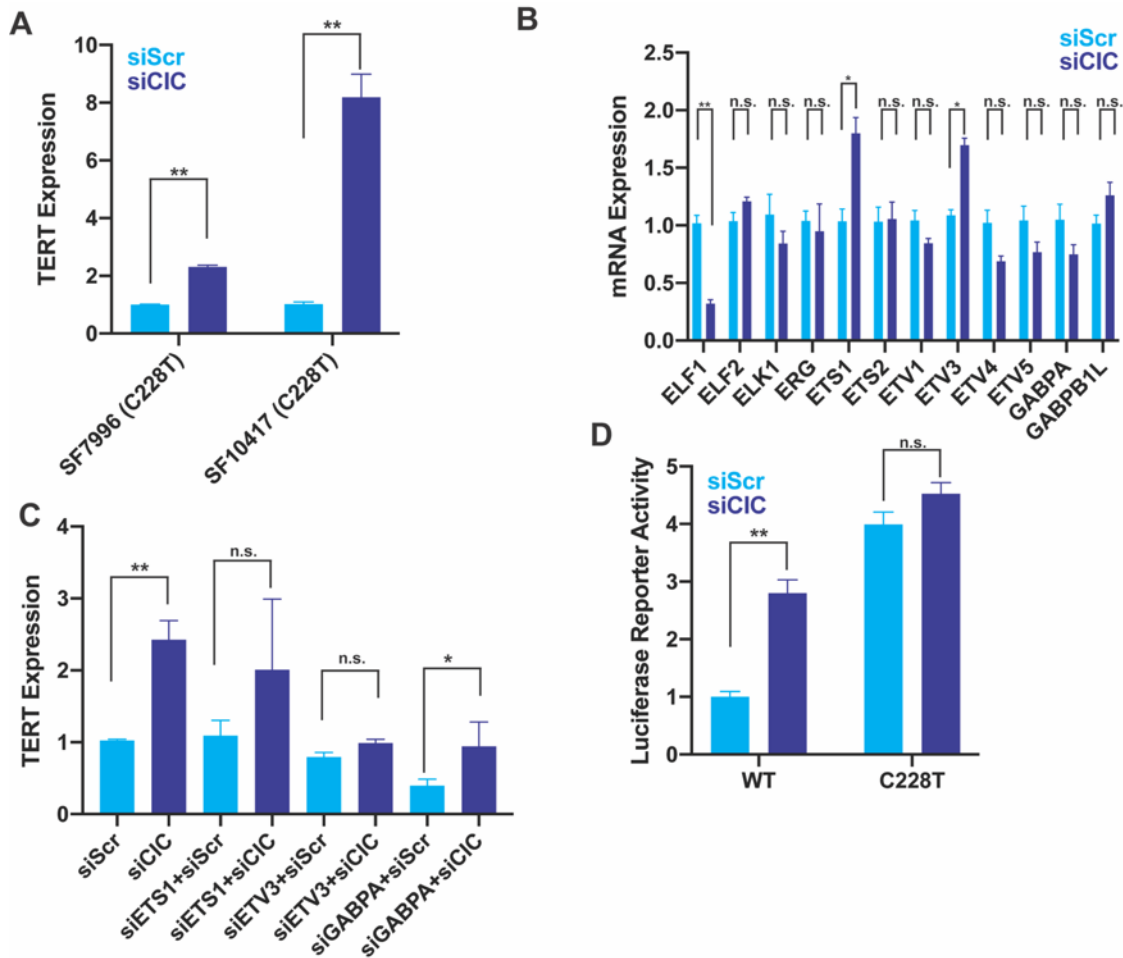


Figure 4.2 CIC regulates the mutant *TERTp* through ETS regulation

(A) *TERT* expression upon siRNA measured by RT-qPCR in GBM (SF7996) and oligodendroglioma (SF10417) cell lines, normalized relative to siScr in each cell line. (B) ETS factor expression upon siRNA measured by RT-qPCR in oligodendroglioma (SF10417), normalized relative to siScr in each gene measured. (C) *TERT* expression upon combinatorial siRNA of CIC with different ETS factors measured by RT-qPCR in oligodendroglioma (SF10417) cell lines, normalized relative to siScr alone. (D) *TERTp*-luciferase reporter assays in SF7996 cells after 72 hours of siRNA knockdown of CIC. Data are normalized relative to siScr treated WT reporter. (A-D), Student's t-tests, two-tailed. * $P < 0.05$, ** $P < 0.005$, data represent mean \pm SEM

CHAPTER 5: CONCLUSIONS

While cell proliferation and telomerase activity are positively correlated in many cancer types, the molecular pathways linking these key tumor phenotypes are poorly understood, particularly in glioma. Our study begins to elucidate the molecular pathways linking *EGFR* amplification, a common and potent driver of proliferation in GBM, and *CIC* mutations in oligodendroglioma to *TERT*_p mutations. This links two of the most common genetic events in GBM and oligodendroglioma respectively and demonstrates the cooperation of receptor tyrosine kinase signaling with *TERT*_p mutations in telomere maintenance. In GBM, the transcription factor GABP appears to be a central connection in this linkage, receiving signals from EGFR through AMPK and activating *TERT* expression, the rate limiting factor in telomerase activity. Meanwhile, *CIC* inactivation appears to modulate the *TERT*_p in a non-mutant specific manner, suggesting pathways feeding into other ETS factors could also be used to target cancer cells. Investigation into signaling through other oncogenic pathways that drive glioma could reveal additional links to the mutant *TERT*_p. For example, AMPK is also activated by *KRAS* overexpression or *PTEN* knockdown in GBM (Chhipa et al 2018), and *KRAS* mutation or amplification is found in ~3% of GBM while *PTEN* alteration is in ~40% of GBM, including in roughly 50% of EGFR amplified cases (Brennan et al 2013). Whether these genetic alterations result in activation of AMPK-GABP-*TERT* alone, or together with *EGFR* amplification is currently unknown. Given serum starvation reduced *TERT* expression in the most common *TERT*_p mutant cancers (**Figure 1.1D**), it is possible unique drivers of proliferation regulate *TERT* in different genetic and epigenetic backgrounds. In other cancer types, BRAF signaling has been linked to *TERT*_p

mutations. A wider survey of the interaction of oncogenic alterations with *TERT*_p mutations and telomere maintenance is warranted.

Drugs targeting telomerase have long been of interest for cancer treatment, but thus far have been unsuccessful in cancer clinical trials. For example, telomerase inhibitors that target the telomerase RNA template TERC, such as imetelstat, have shown promise in preclinical studies, including in GBM, but failed in clinical trials in part due to “on target” toxicity in normal stem cells with TERC and *TERT* expression (Marian et al 2010; Chiappori et al 2015; Kozloff et al 2010). Our results suggest that targeting EGFR with clinically used inhibitors could reduce telomerase activity in a tumor specific manner, via reduced activity of the mutant *TERT*_p. However, the EGFR inhibitor induced telomerase reduction is unlikely on its own to have a strong and sustained antitumor effect, necessitating the development of combination therapies. Further, therapies targeting *TERT* are limited by the slow rate of telomere attrition before cell death pathways are engaged. Therefore, more immediate targeting of pro-growth pathways could serve a dual role of slowing growth in the immediate term and inducing telomere attrition to induce death more gradually.

*TERT*_p mutations appear to be critical throughout tumorigenesis for ongoing telomere maintenance, making them an attractive cancer-specific therapeutic target (Brastianos et al 2017; Körber et al 2019). In this regard, we recently proposed GABP as a potential therapeutic target in combination with chemotherapy (Mancini et al 2018; Amen et al 2021). Similarly, others have demonstrated that gene editing of the mutant *TERT*_p reverses cellular immortality (Li et al 2020). Identifying druggable kinases upstream of the GABP-*TERT* axis such as EGFR and AMPK could facilitate future

targeting of telomere maintenance, though this would require testing combinations with additional approaches to reduce *TERT* to a critically low level that is insufficient to maintain telomeres as tumor cells proliferate. EGFR targeting has not yet proven effective in GBM, which may in part be due to intratumoral heterogeneity (**Figure 3.1D**) (Sottoriva et al 2013). Along these lines, it is also important to identify approaches that will more rapidly induce telomere dysfunction, that are less dependent on relatively long periods of cell division in the absence of *TERT* for telomere reduction and tumor cell killing.

*TERT*_p mutations activate *TERT* to maintain telomeres, but generally at a shorter length relative to other telomere maintenance mechanisms such as alternative lengthening of telomeres in *ATRX* mutant glioma. Telomere dysfunction is associated with chromosomal instability, genome reduplication, chromothripsis, and subsequent focal amplifications or deletions (Chin et al 1999; Davoil et al 2010; Saretzki et al 1999). Recent work has suggested that chromosomal abnormalities encompassing the genes driving proliferation, including gain of chromosome 7 where *EGFR* resides, precede *TERT*_p mutations in GBM, and that *TERT*_p mutations are necessary for clonal expansion (Körber et al 2019). The early placement of *EGFR* copy number gains and *TERT*_p mutations on the evolutionary timescale of GBM development highlights the important role of this duet in the classical subtype of *IDH1*-WT GBM. That *TERT*_p mutations are necessary for clonal expansion suggests that telomere maintenance is also required by pre-cancer cells to overcome replicative senescence in cells that have acquired strong drivers such as EGFR activation through amplification or copy number gain. Meanwhile, *CIC* mutations occur relatively late and are often subclonal (Glietze et

al, 2015), suggesting that cooperative events with the *TERT*_p mutation to elevate *TERT* expression may be more necessary for clonal expansion in some cancers than in others. Consistent with previous models *TERT*_p mutations on their own could endow a sufficient amount of telomerase activity to enable the maintenance of the shortest telomeres (Chiba et al, 2015), which may be sufficient for tumor presentation in less proliferative tumors such as oligodendroglioma.

CHAPTER 6: MATERIALS AND METHODS

Quantitative PCR

RNA was collected with Cells-to-CT kit (ThermoFisher Scientific, #4402955) and reverse transcribed per kit conditions for high throughput (96 well) applications. For low throughput applications, RNA was isolated via Zymo Research Quick-RNA Microprep (#R1051) and cDNA was prepared from 333ng RNA with iScript cDNA Synthesis Kit (Bio-Rad #1708891). qPCR was performed with PowerSybr Green PCR MasterMix (4368577) on an Applied Biosystems QuantStudio 5 Real-Time PCR System. Relative expression levels were calculated by $2^{-\Delta\Delta C_t}$ analysis and normalized within each replicate to control condition.

Western Blotting

Protein was harvested using M-PER Mammalian Protein Extraction Reagent (ThermoFisher #78501) supplemented with Turbonuclease (Sigma-Aldrich #T4330) and Halt Protease and Phosphatase Inhibitor (ThermoFisher #78446). Protein was quantified with a BCA assay (ThermoFisher #23225) 20-40 μ g of protein was loaded into NuPAGE Tris-Acetate 3-8% gels (EA0375) and separated via electrophoresis on XCell SureLock Mini-Cell before transfer to Immobilon PVDF Membrane (Millipore #IPVH00010) in XCell II Blot Module. Blocking, primary, and secondary antibody incubation was performed in 5% BSA in 0.1% Tween-20 tris buffered saline (Sigma-Aldrich A9647). Membranes were incubated for 5 minutes in ECL Western Blotting Substrate (ThermoFisher #32109) before chemiluminescent detection with x-ray film. Background-subtracted signal was quantified via densitometry using ImageJ software.

Chromatin Immunoprecipitation

ChIP was performed using the ActiveMotif ChIP-IT High Sensitivity kit (ActiveMotif #53040). Cells were grown in two 15 cm plates per condition to 80% confluency and fixed using 4% paraformaldehyde. ChIP was performed for GABPA (Millipore Sigma: ABE1047) antibody or IgG isotype control (Cell Signaling Technologies: 2729) using 30µg of chromatin per immunoprecipitation reaction. qPCR was performed using ssoAdvanced Universal SYBR Green Supermix (Biorad #1725270) supplemented with 1M of Resolution Solution from Roche GC-Rich PCR System (Roche #12140306001). qPCR was performed on an Applied Biosystems QuantStudio 5 Real-Time PCR System.

Culturing Human Tumor Cell Lines

Cell lines and patient-derived cultures were grown in a 37°C incubator at 5% CO₂. SF7996, LN229, U251, and LN18 were cultured in DMEM/Ham's F-12 1:1 supplemented with 10% Hyclone FBS (GE Life Sciences #SH30071) and 1% Pen-Strep (Gibco #15140-122). NHAPC5 were grown in DMEM (Corning # 10-013-CV) supplemented with 10% FBS and 1% Pen-Strep as previously described (Mancini et al 2018; Amen et al 2021). GBM6 tumor-sphere cultures (Sarkaria et al 2006) were maintained in sterile-filtered Neurocult-A (StemCell #05751) supplemented with GlutaMAX (Gibco #32050-061), sodium pyruvate (11360-070), N2 (Gibco #17502-048), and B27-A (Gibco #12587-010), and fed twice weekly with 20ng/mL EGF (Peprotech #AF-100-15) and 20 ng/mL FGF (Peprotech #100-18C). All lines were mycoplasma

tested and STR validated upon acquisition as previously described (Mancini et al 2018; Amen et al 2021).

CRISPR sgRNA Design and Editing

sgRNAs were designed using GuideScan 1.0 (Perez et al 2017). To generate full gene knockouts, pairs of guides were chosen flanking the coding region. Guides were subcloned into pSpCas9(BB)-2A-Puro (PX459) V2.0 (Addgene #62988). 250ng of each guide were transfected in tandem with 1.5µL XtremeGene-HP DNA Transfection Reagent. Cells were selected in 1 µg/mL puromycin for 48 hours. 6 pairs of guides (three 5' sgRNA and two 3' sgRNA) were screened by PCR after bulk transfection for editing efficiency and one pair was selected for clone generation. Cells were plated in 96 wells at a concentration of 0.5 cells/100 µL for clone generation.

Clones were screened by PCR with Q5 High-Fidelity DNA Polymerase (NEB #M0491). Separate PCRs were performed for wildtype and deleted alleles using the same forward primer. For wildtype alleles, one primer was nested within the gene. For deleted alleles, the primers flanked the entire gene. Clones were then screened by mRNA and protein, compared to parental cells, for loss of expression.

TCGA and MSK-IMPACT Data Access

Processed TCGA RNA-Seq, RPPA, and GISTIC copy number data as well as processed hybridization capture-based mutation and copy number information from MSK-IMPACT was accessed via cBioPortal (Cerami et al 2012; Gao et al 2013).

Spatially Mapped Sample Collection and Data Processing

University of California, San Francisco's Institutional Review Board approved sample collection and usage. Spatially mapped sample coordinates were acquired by a neurosurgeon using Brainlab Cranial Navigation software, which records sample coordinates on a preoperative MRI. T2/FLAIR MRI was used to preoperatively define the tumor lesion. 3D models of the tumor based on T2/FLAIR images were constructed using Slicer software.

Exome capture was performed using Nimblegen SeqCap EZ Exome v3. Tumor cell purity was estimated using FACETS from whole exome sequencing data (Shen and Shesan 2016). RNA-seq data from multi-sample human GBM was performed as previously described. Briefly, genomic DNA and RNA were extracted from the same tissue sample using an AllPrep DNA/RNA/miRNA Universal Kit (Qiagen #80234). Libraries were prepared using the Kapa Stranded mRNA-Seq Kit (Kapa Biosystems #KR0960-v2.14). Sequencing was performed on either a HiSeq2000, HiSeq4000, or NovaSeq. Alignment to hg19 was performed with TopHat v2.0.12 using a GENCODE V19 transcriptome-guided alignment and featureCounts v1.4.6 was used to calculate reads per gene. Previously uploaded whole exome sequencing and RNA sequencing libraries can be accessed in the European Genome-Phenome Archive under the accession number EGA00001003710.

Plasmids

PRKAB1 (#1:TRCN0000004770 and #2:TRCN0000004771), EGFR (#1:TRCN00000010329 and #2 TRCN00000039634) and non-targeting control shRNA (SHC016) were purchased from Sigma MISSION shRNA. The constitutive lentiviral vector, N174-MCS-puro (Addgene #81068), was modified into a robust RNAi system through a sequential cloning process to contain a single CMV promoter driving expression of the TurboGFP-miR-E-IRES-puro transcript. This lenti-RNAi system employed a single CMV promoter and IRES to achieve a homogenous population of cells with efficient knockdown following transduction and puromycin selection. The miR-E shRNAs were designed using the online portal Splash RNA (<http://splashrna.mskcc.org/>) (Pelossof et al 2017) with advanced settings changed to 6 predictions per gene and the input consisting of either the refseq ID or FASTA mRNA sequence. EGFRvIII CDS was synthesized by Twist Bioscience and subcloned into pCW57.1-MCS1-P2A-MCS2 Neo (Addgene #89180) for doxycycline-inducible expression. pDONR223-PRKAA2 (Addgene #23671) was cloned into pLX301 (Addgene #25895) with Gateway LR Clonase II Enzyme Mix (ThermoFisher #11791020). PRKAA2-D157A was generated using QuikChange Lightning Site Directed Mutagenesis Kit (Agilent #210518). *TERT* CDS was subcloned into N174-UBC-Int1-MCS-IRES-Neo.

Lentiviral production

Lentivirus was produced in 293T using second generation packaging plasmids, envelope plasmid pMD2.G (Addgene #12259) and packaging plasmid psPAX2 (Addgene #12260). Particles were prepared in 6 well plates using transfection reactions

of 1 µg transfer vector, 0.75 µg packaging vector and 0.25 µg envelope vector in serum free media with addition of 0.6 µL XtremeGene-HP DNA Transfection Reagent (Roche # 6366546001) for a 3:1 molar ratio. Media was changed 12-16 hours after transfection and virus was harvested 48 hours later. Viral supernatant was filtered through 0.2 µm polyethersulfone membrane filters (ThermoFisher #720-1320). Selection of stable cell lines was performed for 24 hours after viral transduction under 0.5-1 µg/mL puromycin (ThermoFisher #A1113803) or 500ng/mL G418 (ThermoFisher #10131035) as applicable.

Luciferase reporter assays

WT (Addgene #84924), C228T (Addgene #84926), and C250T (Addgene #84925) *TERT* luciferase reporter constructs were used as previously described with Dual-Luciferase Reporter Assay System (Promega #E1910)¹⁵. Briefly, 3000 cells/well were plated into 96 well white plates and transfected 24 hours later with 90ng *TERT* reporter vector, 9ng pGL4.74 and 0.3 µL XtremeGene-HP DNA Transfection Reagent and read 48 hours later. Each condition was plated into six wells for each of three biological replicates.

siRNA knockdown

siGENOME SMARTpools were purchased from Dharmacon—non-targeting (D-00206-13-20), GABPA (M-011662-01), and PRKAB1 (M-007675-00-0005). Cells were transfected with a molar ratio of 5:1 siRNA to Dharmafect 1 and harvested 72 hours post-transfection.

Telomerase Repeat Amplification Protocol

TRAP assays were performed as previously described (Mender and Shay 2015), at a concentration of 2,500 cells/uL. 1 uL lysate was used for each amplification, with 1uL NP-40 lysis buffer serving as a negative control. Oligonucleotides were synthesized by Integrated DNA Technologies. Cy5 signal was visualized on a BioRad ChemiDoc Imager and background-subtracted signal was quantified via densitometry using ImageJ software.

Telomere Restriction Fragmentation (TRF)

Telomere restriction fragmentation was performed using the TeloTAGGG Telomere Length Assay Kit (Roche 12209136001). 1-1.5 µg restricted genomic DNA was separated in 0.8% Ultra High MW agarose in TAE for 2 to 4 hrs. Gels were incubated with 0.5% HCl and denatured and neutralized as per kit conditions. After overnight transfer to nylon membrane with 20x SSC, the DNA was crosslinked using UV before proceeding with kit protocol.

Statistics

For testing of significance, two-tailed student's t-tests were used for RT-qPCR, western blotting, and luciferase assays for three separate biological replicates. For TCGA analyses, Wilcoxon rank-sum tests were used. P values <.05 were considered significant. For association between EGFR amplification and *TERT*_p mutations, a two-tailed Fisher exact probability test was utilized. For comparisons between three or more conditions, a one-way ANOVA was performed to test for global significance. If

significance was reached, individual two-tailed student's t-tests were used. Significance tests were performed using GraphPad Prism 9 software.

Table 1.1 List of Reagents and Primers Used

Antibodies			
Target	Company	Catalog Number	
p-EGFR (Y)	Cell Signaling Technology	2234S	
EGFR	Cell Signaling Technology	4267S	
GABPA	Millipore Sigma	ABE1047	
GABPB1	Proteintech	12597-1-AP	
GAPDH	Millipore Sigma	CB1001	
p-AMPKA (T)	Cell Signaling Technology	2535S	
AMPKA1/2	Cell Signaling Technology	2532S	
AMPKB1/2	Cell Signaling Technology	4150S	
anti-Rabbit I	Cell Signaling Technology	7074S	
anti-Mouse I	Cell Signaling Technology	7070S	
shRNA Sequences			
Target	Sequence	Source	Catalog Number
PRKAB1_1	GCCTGGCTATGGAACTAAATA	MISSION Sigma	TRCN0000004770
PRKAB1_2	CCTCACCAGAAGCCACAATAA	MISSION Sigma	TRCN0000004771
EGFR_1	GAGAATGTGGAATACCTAAGG	MISSION Sigma	TRCN0000010329
EGFR_2	GCTGGATGATAGACGCAGATA	MISSION Sigma	TRCN0000039634
non-targetin	GCGCGATAGCGCTAATAATTT	MISSION Sigma	SHC016
PPP1R12C (C	TTATCTCGAAAATACCTTCTCC	SplashRNA	
TERT	TGACATAAAAGAAAGACCTGAG	SplashRNA	
qPCR Gene Expression Primers			
	Forward	Reverse	
GUSB	CTCATTGGAATTTTGCCGATT	CCGAGTGAAGATCCCCTTTTTA	
TERT	TCACGGAGACCACGTTTCAAA	TTCAAGTGCTGTCTGATTCCAAT	
GABPB1	TCCACTTCATCTAGCAGCACA	GTAATGGTGTTCGGTCCACTT	
GABPA	AAGAACGCCTTGGGATACCCT	GTGAGGTCTATATCGGTCATGCT	
EGFR	TTGCCGCAAAGTGTGTAACG	GTCACCCCTAAATGCCACCG	
PRKAB1	CCACTCCGAGGAAATCAAGGC	CTGGGCGGGAGCTTTATCA	
CRISPR Guides and Sequencing Primers			
sgRNA			
PRKAB1_5'	TGGCCATAAGACGCCCCGGA		
PRKAB1_3'	TGGTGCTCAGCGCAACCCAC		
Primers			
PRKAB1_For	GTAAAGCGCGATTGCGAGAG		
PRKAB1_WT	CCCTCTCCGTTCTGGTGTIT		
PRKAB1_tKO	CTCAACAGGGACAAGTGGCT		

ChIP qPCR Primers			
	Forward	Reverse	
TERT Promot	GCCGGGGCCAGGGCTTCCA	CCGCGCTTCCCACGTGGCGG	

REFERENCES

Aibaidula A, Chan AK-Y, Shi Z, Li Y, Zhang R, Yang R, Li KK-W, Chung NY-F, Yao Y, Zhou L, et al. 2017. Adult IDH wild-type lower-grade gliomas should be further stratified. *Neuro Oncol* **19**: 1327–1337.

Amen AM, Fellmann C, Soczek KM, Ren SM, Lew RJ, Knott GJ, Park JE, McKinney AM, Mancini A, Doudna JA, et al. 2021. Cancer-specific loss of TERT activation sensitizes glioblastoma to DNA damage. *PNAS* **118**.

Aquilanti E, Kageler L, Wen PY, Meyerson M. 2021. Telomerase as a therapeutic target in glioblastoma. *Neuro-Oncology*.

Arita H, Narita Y, Fukushima S, Tateishi K, Matsushita Y, Yoshida A, Miyakita Y, Ohno M, Collins VP, Kawahara N, et al. 2013. Upregulating mutations in the TERT promoter commonly occur in adult malignant gliomas and are strongly associated with total 1p19q loss. *Acta Neuropathol* **126**: 267–276.

Batra SK, Castelino-Prabhu S, Wikstrand CJ, Zhu X, Humphrey PA, Friedman HS, Bigner DD. 1995. Epidermal growth factor ligand-independent, unregulated, cell-transforming potential of a naturally occurring human mutant EGFRvIII gene. *Cell Growth Differ* **6**: 1251–1259.

Bell RJA, Rube HT, Kreig A, Mancini A, Fouse SD, Nagarajan RP, Choi S, Hong C, He D, Pekmezci M, et al. 2015. The transcription factor GABP selectively binds and activates the mutant TERT promoter in cancer. *Science* **348**: 1036–1039.

Bell RJA, Rube HT, Xavier-Magalhães A, Costa BM, Mancini A, Song JS, Costello JF. 2016. Understanding TERT Promoter Mutations: A Common Path to Immortality. *Mol Cancer Res* **14**: 315–323.

Bellon M, Nicot C. 2008. Regulation of Telomerase and Telomeres: Human Tumor Viruses Take Control. *JNCI: Journal of the National Cancer Institute* **100**: 98–108.

Bermudez Y, Yang H, Cheng JQ, Kruk PA. 2008. Pyk2/ERK 1/2 mediate Sp1- and c-Myc-dependent induction of telomerase activity by epidermal growth factor. *Growth Factors* **26**: 1–11.

Bodnar AG, Ouellette M, Frolkis M, Holt SE, Chiu C-P, Morin GB, Harley CB, Shay JW, Lichtsteiner S, Wright WE. 1998. Extension of Life-Span by Introduction of Telomerase into Normal Human Cells. *Science* **279**: 349–352.

Brastianos PK, Nayyar N, Rosebrock D, Leshchiner I, Gill CM, Livitz D, Bertalan MS, D'Andrea M, Hoang K, Aquilanti E, et al. 2017. Resolving the phylogenetic origin of glioblastoma via multifocal genomic analysis of pre-treatment and treatment-resistant autopsy specimens. *npj Precision Onc* **1**: 33.

Brennan CW, Verhaak RGW, McKenna A, Campos B, Noushmehr H, Salama SR, Zheng S, Chakravarty D, Sanborn JZ, Berman SH, et al. 2013. The Somatic Genomic Landscape of Glioblastoma. *Cell* **155**: 462–477.

Bunda S, Heir P, Metcalf J, Li ASC, Agnihotri S, Pusch S, Yasin M, Li M, Burrell K, Mansouri S, et al. 2019. CIC protein instability contributes to tumorigenesis in glioblastoma. *Nat Commun* **10**: 661.

Cerami E, Gao J, Dogrusoz U, Gross BE, Sumer SO, Aksoy BA, Jacobsen A, Byrne CJ, Heuer ML, Larsson E, et al. 2012. The cBio cancer genomics portal: an open platform for exploring multidimensional cancer genomics data. *Cancer Discov* **2**: 401–404.

Cha Y, Kwon SJ, Seol W, Park K-S. 2008. Estrogen receptor-alpha mediates the effects of estradiol on telomerase activity in human mesenchymal stem cells. *Mol Cells* **26**: 454–458.

Chhipa RR, Fan Q, Anderson J, Muraleedharan R, Huang Y, Ciraolo G, Chen X, Waclaw R, Chow LM, Khuchua Z, et al. 2018. AMP kinase promotes glioblastoma bioenergetics and tumour growth. *Nat Cell Biol* **20**: 823–835.

Chiappori AA, Kolevska T, Spigel DR, Hager S, Rarick M, Gadgeel S, Blais N, Pawel JV, Hart L, Reck M, et al. 2015. A randomized phase II study of the telomerase inhibitor imetelstat as maintenance therapy for advanced non-small-cell lung cancer. *Annals of Oncology* **26**: 354–362.

Chiba K, Johnson JZ, Vogan JM, Wagner T, Boyle JM, Hockemeyer D. 2015. Cancer-associated TERT promoter mutations abrogate telomerase silencing ed. T. De Lange. *eLife* **4**: e07918.

Chin L, Artandi SE, Shen Q, Tam A, Lee S-L, Gottlieb GJ, Greider CW, DePinho RA. 1999. p53 Deficiency Rescues the Adverse Effects of Telomere Loss and Cooperates with Telomere Dysfunction to Accelerate Carcinogenesis. *Cell* **97**: 527–538.

Chittaranjan S, Chan S, Yang C, Yang KC, Chen V, Moradian A, Firme M, Song J, Go NE, Blough MD, et al. 2014. Mutations in CIC and IDH1 cooperatively regulate 2-hydroxyglutarate levels and cell clonogenicity. *Oncotarget* **5**: 7960–7979.

Counter CM, Avilion AA, LeFeuvre CE, Stewart NG, Greider CW, Harley CB, Bacchetti S. 1992. Telomere shortening associated with chromosome instability is arrested in immortal cells which express telomerase activity. *The EMBO Journal* **11**: 1921–1929.

Davoli T, Denchi EL, Lange T de. 2010. Persistent Telomere Damage Induces Bypass of Mitosis and Tetraploidy. *Cell* **141**: 81–93.

Brousse FC de la, Birkenmeier EH, King DS, Rowe LB, McKnight SL. 1994. Molecular and genetic characterization of GABP beta. *Genes Dev* **8**: 1853–1865.

Eckel-Passow JE, Lachance DH, Molinaro AM, Walsh KM, Decker PA, Sicotte H, Pekmezci M, Rice T, Kosel ML, Smirnov IV, et al. 2015. Glioma Groups Based on 1p/19q, IDH, and TERT Promoter Mutations in Tumors. *N Engl J Med* **372**: 2499–2508.

Faubert B, Boily G, Izreig S, Griss T, Samborska B, Dong Z, Dupuy F, Chambers C, Fuerth BJ, Viollet B, et al. 2013. AMPK Is a Negative Regulator of the Warburg Effect and Suppresses Tumor Growth In Vivo. *Cell Metabolism* **17**: 113–124.

Gabler L, Lötsch D, Kirchhofer D, van Schoonhoven S, Schmidt HM, Mayr L, Pirker C, Neumayer K, Dinhof C, Kastler L, et al. 2019. TERT expression is susceptible to BRAF and ETS-factor inhibition in BRAFV600E/TERT promoter double-mutated glioma. *Acta Neuropathologica Communications* **7**: 128.

Gao J, Aksoy BA, Dogrusoz U, Dresdner G, Gross B, Sumer SO, Sun Y, Jacobsen A, Sinha R, Larsson E, et al. 2013. Integrative analysis of complex cancer genomics and clinical profiles using the cBioPortal. *Sci Signal* **6**: p11.

Gleize V, Alentorn A, Connen de Kérillis L, Labussière M, Nadaradjane AA, Mundwiller E, Ottolenghi C, Mangesius S, Rahimian A, Ducray F, et al. 2015. CIC inactivating mutations identify aggressive subset of 1p19q codeleted gliomas. *Annals of Neurology* **78**: 355–374.

Greider CW, Blackburn EH. 1985. Identification of a specific telomere terminal transferase activity in tetrahymena extracts. *Cell* **43**: 405–413.

Han F, Li C-F, Cai Z, Zhang X, Jin G, Zhang W-N, Xu C, Wang C-Y, Morrow J, Zhang S, et al. 2018. The critical role of AMPK in driving Akt activation under stress, tumorigenesis and drug resistance. *Nature Communications* **9**: 4728.

Helbing CC, Wellington CL, Gogela-Spehar M, Cheng T, Pinchbeck GG, Johnston RN. 1998. Quiescence versus apoptosis: Myc abundance determines pathway of exit from the cell cycle. *Oncogene* **17**: 1491–1501.

Hiyama K, Hirai Y, Kyoizumi S, Akiyama M, Hiyama E, Piatyszek MA, Shay JW, Ishioka S, Yamakido M. 1995. Activation of telomerase in human lymphocytes and hematopoietic progenitor cells. *The Journal of Immunology* **155**: 3711–3715.

Hoffmeyer K, Raggioli A, Rudloff S, Anton R, Hierholzer A, Valle ID, Hein K, Vogt R, Kemler R. 2012. Wnt/ β -Catenin Signaling Regulates Telomerase in Stem Cells and Cancer Cells. *Science* **336**: 1549–1554.

Holt SE, Aisner DL, Shay JW, Wright WE. 1997. Lack of cell cycle regulation of telomerase activity in human cells. *PNAS* **94**: 10687–10692.

Holt SE, Wright WE, Shay JW. 1996. Regulation of telomerase activity in immortal cell lines. *Mol Cell Biol* **16**: 2932–2939.

Horn S, Figl A, Rachakonda PS, Fischer C, Sucker A, Gast A, Kadel S, Moll I, Nagore E, Hemminki K, et al. 2013. TERT promoter mutations in familial and sporadic melanoma. *Science* **339**: 959–961.

Hsu C-P, Lee L-W, Tang S-C, Hsin I-L, Lin Y-W, Ko J-L. 2015. Epidermal growth factor activates telomerase activity by direct binding of Ets-2 to hTERT promoter in lung cancer cells. *Tumour Biol* **36**: 5389–5398.

Huang FW, Hodis E, Xu MJ, Kryukov GV, Chin L, Garraway LA. 2013. Highly Recurrent TERT Promoter Mutations in Human Melanoma. *Science* **339**: 957–959.

Huang H-JS, Nagane M, Klingbeil CK, Lin H, Nishikawa R, Ji X-D, Huang C-M, Gill GN, Wiley HS, Cavenee WK. 1997. The Enhanced Tumorigenic Activity of a Mutant Epidermal Growth Factor Receptor Common in Human Cancers Is Mediated by Threshold Levels of Constitutive Tyrosine Phosphorylation and Unattenuated Signaling*. *Journal of Biological Chemistry* **272**: 2927–2935.

Huang M, Zeki J, Sumarsono N, Coles GL, Taylor JS, Danzer E, Bruzoni M, Hazard FK, Lacayo NJ, Sakamoto KM, et al. 2020. Epigenetic Targeting of TERT-Associated Gene Expression Signature in Human Neuroblastoma with TERT Overexpression. *Cancer Res* **80**: 1024–1035.

Inoki K, Ouyang H, Zhu T, Lindvall C, Wang Y, Zhang X, Yang Q, Bennett C, Harada Y, Stankunas K, et al. 2006. TSC2 integrates Wnt and energy signals via a coordinated phosphorylation by AMPK and GSK3 to regulate cell growth. *Cell* **126**: 955–968.

Jones RG, Plas DR, Kubek S, Buzzai M, Mu J, Xu Y, Birnbaum MJ, Thompson CB. 2005. AMP-activated protein kinase induces a p53-dependent metabolic checkpoint. *Mol Cell* **18**: 283–293.

Katreddy RR, Bollu LR, Su F, Xian N, Srivastava S, Thomas R, Dai Y, Wu B, Xu Y, Rea MA, et al. 2018. Targeted reduction of the EGFR protein, but not inhibition of its kinase activity, induces mitophagy and death of cancer cells through activation of mTORC2 and Akt. *Oncogenesis* **7**.

Killela PJ, Reitman ZJ, Jiao Y, Bettegowda C, Agrawal N, Diaz LA, Friedman AH, Friedman H, Gallia GL, Giovannella BC, et al. 2013. TERT promoter mutations occur frequently in gliomas and a subset of tumors derived from cells with low rates of self-renewal. *Proc Natl Acad Sci U S A* **110**: 6021–6026.

Kim NW, Piatyszek MA, Prowse KR, Harley CB, West MD, Ho PL, Coviello GM, Wright WE, Weinrich SL, Shay JW. 1994. Specific association of human telomerase activity with immortal cells and cancer. *Science* **266**: 2011–2015.

Körber V, Yang J, Barah P, Wu Y, Stichel D, Gu Z, Fletcher MNC, Jones D, Hentschel B, Lamszus K, et al. 2019. Evolutionary Trajectories of IDHWT Glioblastomas Reveal a Common Path of Early Tumorigenesis Instigated Years ahead of Initial Diagnosis. *Cancer Cell* **35**: 692-704.e12.

Kozloff M, Sledge GW, Benedetti FM, Starr A, Wallace JA, Stuart MJ, Gruver D, Miller K. 2010. Phase I study of imetelstat (GRN163L) in combination with paclitaxel (P) and bevacizumab (B) in patients (pts) with locally recurrent or metastatic breast cancer (MBC). *JCO* **28**: 2598–2598.

Kyo S, Takakura M, Kanaya T, Zhuo W, Fujimoto K, Nishio Y, Orimo A, Inoue M. 1999. Estrogen activates telomerase. *Cancer Res* **59**: 5917–5921.

Kyo S, Takakura M, Kohama T, Inoue M. 1997. Telomerase Activity in Human Endometrium. *Cancer Res* **57**: 610–614.

Labussière M, Boisselier B, Mokhtari K, Stefano A-LD, Rahimian A, Rossetto M, Ciccarino P, Saulnier O, Paterra R, Marie Y, et al. 2014. Combined analysis of TERT, EGFR, and IDH status defines distinct prognostic glioblastoma classes. *Neurology* **83**: 1200–1206.

Lansdorp PM, Verwoerd NP, van de Rijke FM, Dragowska V, Little M-T, Dirks RW, Raap AK, Tanke HJ. 1996. Heterogeneity in Telomere Length of Human Chromosomes. *Human Molecular Genetics* **5**: 685–691.

Li X, Qian X, Wang B, Xia Y, Zheng Y, Du L, Xu D, Xing D, DePinho RA, Lu Z. 2020. Programmable base editing of mutated TERT promoter inhibits brain tumour growth. *Nat Cell Biol* **22**: 282–288.

Li Y, Cheng HS, Chng WJ, Tergaonkar V. 2016. Activation of mutant TERT promoter by RAS-ERK signaling is a key step in malignant progression of BRAF-mutant human melanomas. *Proc Natl Acad Sci U S A* **113**: 14402–14407.

Liu R, Zhang T, Zhu G, Xing M. 2018. Regulation of mutant TERT by BRAF V600E/MAP kinase pathway through FOS/ GABP in human cancer. *Nature Communications* **9**: 579.

Liu X, Chhipa RR, Nakano I, Dasgupta B. 2014. The AMPK Inhibitor Compound C Is a Potent AMPK-Independent Antiglioma Agent. *Mol Cancer Ther* **13**: 596–605.

Louis DN, Perry A, Reifenberger G, von Deimling A, Figarella-Branger D, Cavenee WK, Ohgaki H, Wiestler OD, Kleihues P, Ellison DW. 2016. The 2016 World Health Organization Classification of Tumors of the Central Nervous System: a summary. *Acta Neuropathol* **131**: 803–820.

Maida Y, Kyo S, Kanaya T, Wang Z, Yatabe N, Tanaka M, Nakamura M, Ohmichi M, Gotoh N, Murakami S, et al. 2002. Direct activation of telomerase by EGF through Ets-mediated transactivation of TERT via MAP kinase signaling pathway. *Oncogene* **21**: 4071–4079.

Makowski MM, Willems E, Fang J, Choi J, Zhang T, Jansen PWTC, Brown KM, Vermeulen M. 2016. An interaction proteomics survey of transcription factor binding at recurrent TERT promoter mutations. *PROTEOMICS* **16**: 417–426.

Mancini A, Xavier-Magalhães A, Woods WS, Nguyen K-T, Amen AM, Hayes JL, Fellmann C, Gapinske M, McKinney AM, Hong C, et al. 2018. Disruption of the β 1L Isoform of GABP Reverses Glioblastoma Replicative Immortality in a TERT Promoter Mutation-Dependent Manner. *Cancer Cell* **34**: 513-528.e8.

Marian CO, Cho SK, Mcellin BM, Maher EA, Hatanpaa KJ, Madden CJ, Mickey BE, Wright WE, Shay JW, Bachoo RM. 2010. The Telomerase Antagonist, Imetelstat, Efficiently Targets Glioblastoma Tumor-Initiating Cells Leading to Decreased Proliferation and Tumor Growth. *Clin Cancer Res* **16**: 154–163.

Mender I, Shay JW. 2015. Telomerase Repeated Amplification Protocol (TRAP). *Bio Protoc* **5**.

Noureen N, Wu S, Lv Y, Yang J, Alfred Yung WK, Gelfond J, Wang X, Koul D, Ludlow A, Zheng S. 2021. Integrated analysis of telomerase enzymatic activity unravels an association with cancer stemness and proliferation. *Nat Commun* **12**: 139.

Ohba S, Mukherjee J, Johannessen T-C, Mancini A, Chow TT, Wood M, Jones L, Mazar T, Marshall RE, Viswanath P, et al. 2016. Mutant IDH1 Expression Drives TERT Promoter Reactivation as Part of the Cellular Transformation Process. *Cancer Res* **76**: 6680–6689.

Ostrom QT, Bauchet L, Davis FG, Deltour I, Fisher JL, Langer CE, Pekmezci M, Schwartzbaum JA, Turner MC, Walsh KM, et al. 2014. The epidemiology of glioma in adults: a “state of the science” review. *Neuro-Oncology* **16**: 896–913.

- Patel B, Taiwo R, Kim AH, Dunn GP. 2020. TERT, a promoter of CNS malignancies. *Neuro-Oncology Advances* **2**.
- Peifer M, Hertwig F, Roels F, Dreidax D, Gartlgruber M, Menon R, Krämer A, Roncaioli JL, Sand F, Heuckmann JM, et al. 2015. Telomerase activation by genomic rearrangements in high-risk neuroblastoma. *Nature* **526**: 700–704.
- Pelossof R, Fairchild L, Huang C-H, Widmer C, Sreedharan VT, Sinha N, Lai D-Y, Guan Y, Premsrirut PK, Tschaharganeh DF, et al. 2017. Prediction of potent shRNAs with a sequential classification algorithm. *Nat Biotechnol* **35**: 350–353.
- Perez AR, Pritykin Y, Vidigal JA, Chhangawala S, Zamparo L, Leslie CS, Ventura A. 2017. GuideScan software for improved single and paired CRISPR guide RNA design. *Nat Biotechnol* **35**: 347–349.
- Quaas A, Oldopp T, Tharun L, Klingefeld C, Krech T, Sauter G, Grob TJ. 2014. Frequency of TERT promoter mutations in primary tumors of the liver. *Virchows Arch* **465**: 673–677.
- Remke M, Ramaswamy V, Peacock J, Shih DJH, Koelsche C, Northcott PA, Hill N, Cavalli FMG, Kool M, Wang X, et al. 2013. TERT promoter mutations are highly recurrent in SHH subgroup medulloblastoma. *Acta Neuropathol* **126**: 917–929.
- Ríos M, Foretz M, Viollet B, Prieto A, Fraga M, Costoya JA, Señarís R. 2013. AMPK activation by oncogenesis is required to maintain cancer cell proliferation in astrocytic tumors. *Cancer Res* **73**: 2628–2638.

Rojas M, Yao S, Lin Y-Z. 1996. Controlling Epidermal Growth Factor (EGF)-stimulated Ras Activation in Intact Cells by a Cell-permeable Peptide Mimicking Phosphorylated EGF Receptor *. *Journal of Biological Chemistry* **271**: 27456–27461.

Sahm F, Koelsche C, Meyer J, Pusch S, Lindenberg K, Mueller W, Herold-Mende C, von Deimling A, Hartmann C. 2012. CIC and FUBP1 mutations in oligodendrogliomas, oligoastrocytomas and astrocytomas. *Acta Neuropathol* **123**: 853–860.

Saretzki G, Sitte N, Merkel U, Wurm RE, von Zglinicki T. 1999. Telomere shortening triggers a p53-dependent cell cycle arrest via accumulation of G-rich single stranded DNA fragments. *Oncogene* **18**: 5148–5158.

Sarkaria JN, Carlson BL, Schroeder MA, Grogan P, Brown PD, Giannini C, Ballman KV, Kitange GJ, Guha A, Pandita A, et al. 2006. Use of an Orthotopic Xenograft Model for Assessing the Effect of Epidermal Growth Factor Receptor Amplification on Glioblastoma Radiation Response. *Clin Cancer Res* **12**: 2264–2271.

Shaw RJ, Bardeesy N, Manning BD, Lopez L, Kosmatka M, DePinho RA, Cantley LC. 2004. The LKB1 tumor suppressor negatively regulates mTOR signaling. *Cancer Cell* **6**: 91–99.

Shay JW, Bacchetti S. 1997. A survey of telomerase activity in human cancer. *Eur J Cancer* **33**: 787–791.

Shen R, Seshan VE. 2016. FACETS: allele-specific copy number and clonal heterogeneity analysis tool for high-throughput DNA sequencing. *Nucleic Acids Res* **44**: e131.

Simon M, Hosen I, Gousias K, Rachakonda S, Heidenreich B, Gessi M, Schramm J, Hemminki K, Waha A, Kumar R. 2015. TERT promoter mutations: a novel independent prognostic factor in primary glioblastomas. *Neuro-Oncology* **17**: 45–52.

Sottoriva A, Spiteri I, Piccirillo SGM, Touloumis A, Collins VP, Marioni JC, Curtis C, Watts C, Tavaré S. 2013. Intratumor heterogeneity in human glioblastoma reflects cancer evolutionary dynamics. *PNAS* **110**: 4009–4014.

Spiegel-Kreinecker S, Lötsch D, Ghanim B, Pirker C, Mohr T, Laaber M, Weis S, Olschowski A, Webersinke G, Pichler J, et al. 2015. Prognostic quality of activating TERT promoter mutations in glioblastoma: interaction with the rs2853669 polymorphism and patient age at diagnosis. *Neuro Oncol* **17**: 1231–1240.

Stein SC, Woods A, Jones NA, Davison MD, Carling D. 2000. The regulation of AMP-activated protein kinase by phosphorylation. *Biochem J* **345**: 437–443.

Stern JL, Theodorescu D, Vogelstein B, Papadopoulos N, Cech TR. 2015. Mutation of the TERT promoter, switch to active chromatin, and monoallelic TERT expression in multiple cancers. *Genes Dev.*

Stupp R, Taillibert S, Kanner A, Read W, Steinberg DM, Lhermitte B, Toms S, Idbaih A, Ahluwalia MS, Fink K, et al. 2017. Effect of Tumor-Treating Fields Plus Maintenance Temozolomide vs Maintenance Temozolomide Alone on Survival in Patients With Glioblastoma: A Randomized Clinical Trial. *JAMA* **318**: 2306–2316.

Vallarelli AF, Rachakonda PS, André J, Heidenreich B, Riffaud L, Bensussan A, Kumar R, Dumaz N. 2016. TERT promoter mutations in melanoma render TERT expression dependent on MAPK pathway activation. *Oncotarget* **7**: 53127–53136.

Vinagre J, Almeida A, Pópulo H, Batista R, Lyra J, Pinto V, Coelho R, Celestino R, Prazeres H, Lima L, et al. 2013. Frequency of TERT promoter mutations in human cancers. *Nat Commun* **4**: 2185.

Whittemore K, Vera E, Martínez-Nevado E, Sanpera C, Blasco MA. 2019. Telomere shortening rate predicts species life span. *PNAS* **116**: 15122–15127.

Wijnenga MMJ, Dubbink HJ, French PJ, Synhaeve NE, Dinjens WNM, Atmodimedjo PN, Kros JM, Dirven CMF, Vincent AJPE, van den Bent MJ. 2017. Molecular and clinical heterogeneity of adult diffuse low-grade IDH wild-type gliomas: assessment of TERT promoter mutation and chromosome 7 and 10 copy number status allows superior prognostic stratification. *Acta Neuropathol* **134**: 957–959.

Yang Z-F, Mott S, Rosmarin AG. 2007. The Ets transcription factor GABP is required for cell-cycle progression. *Nat Cell Biol* **9**: 339–346.

Zehir A, Benayed R, Shah RH, Syed A, Middha S, Kim HR, Srinivasan P, Gao J, Chakravarty D, Devlin SM, et al. 2017. Mutational Landscape of Metastatic Cancer Revealed from Prospective Clinical Sequencing of 10,000 Patients. *Nat Med* **23**: 703–713.

Publishing Agreement

It is the policy of the University to encourage open access and broad distribution of all theses, dissertations, and manuscripts. The Graduate Division will facilitate the distribution of UCSF theses, dissertations, and manuscripts to the UCSF Library for open access and distribution. UCSF will make such theses, dissertations, and manuscripts accessible to the public and will take reasonable steps to preserve these works in perpetuity.

I hereby grant the non-exclusive, perpetual right to The Regents of the University of California to reproduce, publicly display, distribute, preserve, and publish copies of my thesis, dissertation, or manuscript in any form or media, now existing or later derived, including access online for teaching, research, and public service purposes.

DocuSigned by:

Andrew McKinney

C488100BF351473...

Author Signature

2/24/2022

Date